Characterizing the use of differentiated medulloblastoma cells to examine Herpes Simplex Virus latency and reactivation

A Thesis Submitted to the College of
Graduate Studies and Research
in Partial Fulfillment of the Requirements
for the Degree of Master of Science
in the Department of Veterinary Microbiology
University of Saskatchewan
Saskatoon, Canada

By
Kristen Lee Schroeder

Permission to Use

In presenting this thesis in partial fulfillment of the requirements for a Postgraduate degree from the University of Saskatchewan, I agree that the Libraries of this University may make it freely available for inspection. I further agree that permission for copying of this thesis, in any manner, in whole or part, for scholarly purposes may be granted by the professor or professors who supervised my thesis work or, in their absence, by the Head of the Department or the Dean of the College in which my thesis work was done. It is understood that any copying or publication or use of this thesis or parts thereof for financial gain shall not be allowed without my written permission. It is also understood that due recognition shall be given to me and to the University of Saskatchewan in any scholarly use which may be made of any material in my thesis.

Requests for permission to copy or to make other use of material in this thesis in whole or part should be addressed to:

Head of the Department of Veterinary Microbiology
University of Saskatchewan
52 Campus Drive
Saskatoon, Saskatchewan S7N 5B4

Abstract

In human infection, herpes simplex virus (HSV) navigates two distinct life cycles; lytic and latent. The latent cycle takes place in sensory neurons, and is characterized as a dormant period punctuated by stress-induced episodes of viral reactivation. Understanding the mechanisms by which HSV latency and reactivation occur has been hindered by the lack of a model that faithfully recapitulates the environment of a human sensory neuron. Systems ranging from rat neurons to human fibroblasts have been developed to host HSV latency, however few available models have been able to investigate the role of human neuron-specific factors. To address this need, human medulloblastoma tumour cell lines, which derive from neuronal precursor cells, were differentiated and examined for their ability to host the HSV latency-reactivation cycle—in a manner similar to the differentiated PC-12 cell model. ONS-76 and UW228 medulloblastoma cell lines were screened for differentiation capacity. The differentiated cells were demonstrated to possess neuronal character as several neuron-specific proteins were found to be expressed. Differentiated ONS-76 cells were not compatible with hosting HSV latency, however, infection with a viral mutant impaired for lytic cycle initiation exhibited a deviant pattern of gene expression that resembles what has been observed in reactivation. Differentiated UW228 cells were found to host a low frequency, stable infection with the HSV mutant, characterized by the absence of infectious virus and viral lytic gene expression in the presence of persisting viral DNA. This DNA could further be induced to re-enter the lytic cycle through heat shock treatment and removal of differentiating agents from cell cultures. These results depict differentiated medulloblastoma cells as a novel tool in the study of HSV latency and reactivation, as these cells derive from the central nervous system and provide a new cellular perspective through which HSV biology can be viewed.

Keywords: HSV, latency, reactivation, medulloblastoma, VP16

Acknowledgements

I would like to thank Dr. Vikram Misra for his direction and guidance throughout this project. I would also like to thank my committee members Dr. Janet Hill and Dr. Joyce Wilson for their valuable insight and advice. Financial support for this work was provided by an NSERC Discovery grant (awarded to VM), a Department of Veterinary Microbiology devolved scholarship, the WCVM Research Trust fund, and the Saskatchewan Innovation and Opportunity Scholarship, and to these agencies I express my sincerest gratitude. I also wish to extend special appreciation to Noreen Rapin and Andrea Di Marzo for their help with everything from microscopes to bad lab days.

My thanks are extended to lab members past and present, my friends at the college, and all of my professors and advisors through this process. You are too numerous to mention by name but are a community I am very grateful to have been a part of.

Lastly I would like to thank Landon, my friends and family, and the women of the Saskatoon Roller Derby League. Your inspiration and support are legend.

Table of Contents

List of Figures

List of Tables

List of Abbreviations

ACV	acyclovir (acycloguanosine)
Brn3A	brain-specific homeobox/POU domain protein 3A
bp	base pair
cDNA	complementary deoxyribonucleic acid
CNS	central nervous system
CO_2	carbon dioxide
CPE	cytopathic effect
Ct	cycle threshold
DAPI	4'6-diamidino-2-phenylindole
DBcAMP	dibutyryl cyclic adenosine monophosphate
DNA	deoxyribonucleic acid
dNTP	deoxyribonucleotide triphosphate
dpi	days post infection
EDTA	ethylenediaminetetraacetic acid
FBS	fetal bovine serum
GAPDH	glyceraldehyde-3-phosphate dehydrogenase
GFAP	glial fibrillary acidic protein
GMP	glassware and media preparation
HCF	host cell factor 1
HDAC	histone deacetylase
HMBA	hexamethylene bis(acetamide)
hpi	hours post infection
HSV	herpes simplex virus type 1
HVEM	herpesvirus entry mediator
ICP0	infected cell protein 0
ICP4	infected cell protein 4
ICP27	infected cell protein 27
IE	immediate-early

IF	indirect immunofluorescent staining
iPS	induced pluripotent stem cells
kb	kilobase pair
LAT	latency associated transcript
MOI	multiplicity of infection
NBCS	newborn calf serum
ND10	nuclear domain 10
NeuN	neuronal nuclear antigen (Fox-3)
NF	neurofilament
NGF	nerve growth factor
Oct-1	POU domain octamer transcription factor 1 (POU2F1)
PBS	phosphate buffered saline
PBST	phosphate buffered saline + 0.1% Triton-X 100
Pen-strep	penicillin streptomycin
pfu	plaque forming units
PI	propidium iodide
qRT-PCR	quantitative real-time polymerase chain reaction
RNA	ribonucleic acid
SDS	sodium dodecyl sulfate
TBE	tris borate EDTA buffer
TG	trigeminal ganglia
TK	thymidine kinase
TrkA	neurotrophic tyrosine kinase receptor type 1
TSA	trichostatin A
UV	ultraviolet
VIC	VP16-induced complex
VP5	virion protein 5
VP16	virion protein 16
ZF	cyclic AMP responsive element binding protein (Zhangfei)

Chapter 1 Introduction

Herpes simplex virus type 1 (HSV) is a human pathogen that navigates two distinct replicative programs within its host; lytic and latent. In lytic replication the virus rapidly produces progeny via a regulated program of gene expression. By contrast HSV latency features long-term repression of the lytic program that may be punctuated by episodes of stress-induced productive replication, termed reactivation. The lytic replicative cycle has been well defined [1], however the process by which HSV establishes and reactivates from latency is less clear. The difficulty in studying this aspect of HSV biology has primarily come from the lack of a suitable model to host experimental latency, as the virus has adapted to enter this state specifically within the environment of the human neuron. Current understanding of the molecular interplay between neuron and virus is discussed in this section, including a review of the available models of HSV latency and their limitations.

1.1 HSV pathogenesis

HSV is a double-stranded DNA virus that belongs to the *Alphaherpesvirinae* subfamily of *Herpesviridae* and is a pathogen of humans. As with other alphaherpesviruses HSV employs two distinct infectious cycles in its host: a productive or lytic cycle that takes place in mucoepithelial tissues (described in [1]), and a latency-reactivation cycle restricted to sensory neurons of the peripheral nervous system [1]. When HSV encounters a naïve host lytic replication occurs at the body surface, often resulting in development of characteristic lesions. Production of viral progeny at this site feeds the establishment of latency as innervating sensory neurons are infected at the axon terminus. Inside the neuron the virus enters latency, which may be maintained for the life of the host with intermittent episodes of viral reactivation. HSV reactivation can be induced by a variety of stress stimuli, and features the reemergence of infectious virus from the neuron at the axon terminus and infection of epithelial cells at this site. The frequency and severity of recrudescent infection varies between individuals and is thought to depend on factors such as genetic differences in the immune system. The success of establishing a latent reservoir is demonstrated by high seroprevalence rates of HSV in the human population [2].

1.2 Lytic replication

While productive HSV infection occurs primarily in the mucoepithelial tissue of human hosts, the virus can successfully replicate in an extensive range of cell types *in vitro*, including epithelial, fibroblast, and tumour cells from multiple species (reviewed in [3]). The molecular process behind lytic HSV replication has been well described (see [1]) and proceeds by a sequential cascade of expression from three gene classes—immediate-early (IE, α), early (E, β), and late (L, γ). Gene expression is initiated following viral entry and nuclear inoculation by the viral protein VP16, which is imported into the cell as a preformed component of the virion. The VP16-induced complex (VIC) is comprised of VP16 and two cellular cofactors, host cell factor C1 (HCF) and the POU domain octamer transcription factor 1 (Oct-1), and binds a recognition sequence in the IE gene promoters to initiate their transcription [4]. Proteins translated from the IE class genes direct and enhance viral replication and assembly, as well as counteract repression of the virus by the cell [5]. IE proteins activate expression of the early gene class, which encodes machinery for replicating the viral genome. Synthesis of the early proteins and viral DNA replication are followed by activation of expression from the late gene class. The late genes typically encode structural capsid proteins and proteins that must be carried with the virion to initiate infection in a naïve cell [1]. The VP16 protein is synthesized as a late gene product and is assembled into the capsids of progeny virus prior to egress from the cell [6, 7]. The finding that HSV lytic replication is driven by VP16, a late gene product, has complicated the understanding of how reactivation from latency occurs, as expression of all lytic gene classes depends on the presence of earlier gene class products.

As with most viruses, many aspects of the cellular environment are altered by HSV to facilitate its successful replication. Host protein synthesis is attenuated through degradation of cellular mRNA [8], and interference with innate immune function allows for evasion of host defenses (reviewed in [9]). Attempts by the cell to repress the incoming virus through intrinsic mechanisms, such as epigenetic silencing, are also counteracted by HSV during the early stages of replication (reviewed in [10]). Proper function of viral regulatory proteins that enact these processes is important to successful replication, and

how these actions are circumvented in the establishment of latency is key to understanding the dual life cycle of HSV.

1.3 The latency-reactivation cycle

Latent HSV infection occurs in sensory neurons and can be broken into three phases: establishment, where the virus infects the neuron and transitions into the latent state; maintenance, where the virus remains dormant inside the neuron nucleus; and reactivation, where the virus is stimulated to exit latency and produce infectious progeny. HSV latency is defined by the presence of viral DNA in the absence of infectious virus and without transcription of the lytic program, and the ability to provoke reactivation from this persistent DNA. No single mechanism has been identified as the mediator of entrance into or exit from latency, and the latency-reactivation cycle may be regarded as the sum of several interactions between virus and neuron. Current dogma posits that HSV latency is heterogeneous in nature, where the virus is maintained in a more or less repressed state dependent on the environment of the neuron it inhabits. Viral reactivation, provoked by the cellular response to stress, is similarly viewed as a process dependent on the intensity of stress and number of available viral genomes. Molecular mechanisms involved in navigation of the HSV latency-reactivation cycle are summarized in Figure 1.1 and Figure 1.3.

1.3.1 Establishment and maintenance of latency

1.3.1.1 The environment at the site of latency:

Physical differences in the environment encountered by HSV upon entry into a neuron versus epithelial cell may contribute to initiation of viral latency versus lytic replication. Upon entry of the virus into the neuron, the first barrier to initiating lytic infection is navigating transport from the axon terminus to the cell body and nucleus. While VP16 is readily detected in the nucleus of productively infected cells, several studies have demonstrated that this protein dissociates from the virus prior to retrograde axonal transport [11, 12]. As the site of viral entry has been shown to be a determinant of the nuclear presence of VP16 [13] and thus initiation of IE gene expression, this represents a key factor in the decision between productive infection and genome silencing. A second

barrier to activation of the lytic program is the extranuclear localization of HCF specifically in neurons. In latently infected sensory neurons HCF is tethered to the Golgi apparatus [14], physically separated from the virus in the nucleus. In addition, a reported low abundance of Oct-1 in mature neurons [15] and an inability of other POU-domain transcription factors to substitute for Oct-1 in HSV transcription initiation [16, 17] suggest yet a third barrier to assembling the VIC in neurons. Despite these findings HSV is known to undergo an acute phase of productive replication in the trigeminal ganglia (TG) [18, 19], and populations of neurons that have experienced lytic gene expression prior to latency establishment are detectable [20, 21]. These results suggest that partial progression through the lytic program has a limited effect on the ability of HSV to enter latency, however the significance of these observations in view of the neuronal barriers to VIC assembly is not well resolved.

The subtype of neuron encountered by the incoming virus may also play a role in how latent infection is established. This is indicated by the observation that latency is preferentially established in distinct populations of neurons, despite the susceptibility of all neurons to infection [22, 23]. Latency-prone neuron populations are nerve growth factor (NGF)-responsive nociceptors that display a characteristic pattern of immunoreactivity [22, 24], however these biochemical properties have not been linked mechanistically to HSV latency. Variation in HSV copy number between the neurons of infected ganglia also supports the notion of neuron-specific differences making important contributions to the fate of the virus [25]. Collectively these reports illustrate that the physiology and biochemistry of the infected neuron is important to the process of establishing HSV latency.

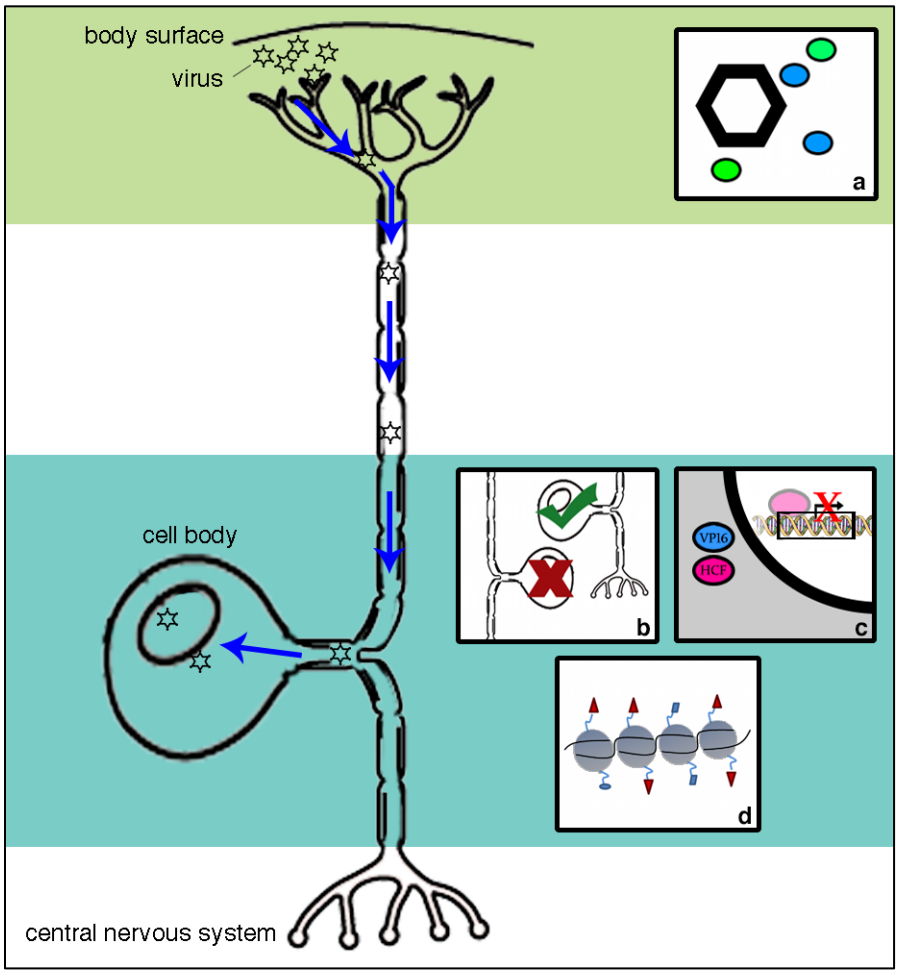

Figure 1.1. Contributing factors in the establishment of HSV latency.
HSV latency is preferentially established within the neuron. a) following viral entry, capsid proteins, including VP16, are lost prior to axonal transport to the nucleus. b) physiological and biochemical differences between neuron subtypes influence HSV to enter latency or undergo lytic replication in the nucleus. c) the absence of VIC components in the nucleus impair induction of the lytic program. d) cellular epigenetic mechanisms load repressive chromatin onto the virus, silencing the lytic program and transitioning the virus into latency. Image credits: neuron adapted from [26], nucleosomes adapted from [27].

1.3.1.2 Transitioning into latency:

Transition of HSV into the latent state involves changes in both the conformation of the viral genome and its association with cellular proteins. HSV is known to circularize as an episome following nuclear import [28], a process that facilitates long-term persistence in the host cell. In addition to this conformational change, the incoming virus is loaded with histones and gradually packaged into a secondary organization resembling cellular heterochromatin [29]. HSV genomes entering the nucleus localize to nuclear domain 10

(ND10) structures, which contain protein effectors that cooperatively repress viral gene expression [30] as well as modulate cellular chromatin dynamics [31]. As entrance into latency progresses, histones associated with the HSV genome accumulate marks of transcriptional silencing [32]. A hallmark of HSV latency is the absence of lytic program transcription, and while some degree of lytic gene expression may occur during establishment [20, 33], once the virus has transitioned into the latent state transcriptional silence prevails.

1.3.1.3 Maintaining latency:

Once HSV has transitioned into a latent state the virus can persist in the neuron indefinitely, maintained by signals from the virus, cell, and immune system. By utilizing input from these sources to enforce latency, the virus is attuned to changes in its environment that may signal a need to initiate reactivation.

One exception to long-term transcriptional silencing of HSV in latency is the region of the latency associated transcript (LAT), an active locus segregated from the repressive chromatin on the remainder of the genome [34]. The primary LAT is an 8.3kb RNA transcript that is processed to yield smaller functional RNA products [35], as well as microRNA species [36]. This transcript has been ascribed many functions during latency, however none are an absolute requirement for latency and reactivation to occur: the phenotype of LAT-deleted viral mutants differs between models but the ability to establish latency and reactivate is generally retained [25, 37]. No LAT protein has been reliably detected, and the transcript is accepted to function as a regulatory RNA. It has been indicated that some products of the primary transcript act through RNA interference pathways [38, 39], while other products may effect epigenetic silencing in a manner similar to other long non-coding RNAs [40]. The most clearly defined function of the LAT is its ability to protect infected cells from apoptosis [41]. The presence of a functional LAT region is associated with decreased apoptosis during HSV infection [42], and the LAT deletion phenotype can be rescued by introducing a cellular anti-apoptotic gene [43]. Expression of the LAT has also been found to vary between neurons carrying latent HSV [44, 45], alluding to the heterogeneous nature of HSV latency.

Cellular signaling also plays a role in maintaining HSV latency, and signaling pathways stimulated by the presence of certain growth factors have been shown to regulate the decision between latency and reactivation. Withdrawal of NGF from *ex vivo* cultured neurons has long been known to induce reactivation of latent HSV [46]. It has since been determined that NGF-mediated activation of the receptor tyrosine kinase TrkA results in stimulation of Akt, a cellular protein involved in a myriad of signaling pathways, and that active signaling through this network is required to maintain HSV latency [47]. This work has demonstrated how input from the cell reinforces the latent state, sensitizing the virus to disruptions in the availability of growth factors via cell signaling cascades.

The influence of the immune system is additionally known to play a role in the maintenance of HSV latency. Latently infected ganglia attract CD8+ T cells [48], which have been shown to strongly inhibit viral replication via nonlethal administration of interferon gamma and granzyme B to the neuron [49]. The LAT may participate in protecting infected neurons from the cytotoxic effects of infiltrating CD8+ T cells [50], indicating yet another level of regulatory virus-cell interaction in latency. Other immune cytokines, such as interferon alpha, have also been reported to aid in the development and maintenance of latency [51]. This presents a mechanism by which HSV latency is maintained via forces external to the neuronal environment, allowing the virus to include the state of the host organism in the decision between maintaining latency and reactivation.

1.3.2 Reactivation

In humans, latent infection is punctuated by episodes of reactivation which culminate in production and spread of infectious virus at the body surface. HSV reactivation frequently follows the experience of stress, such as sunburn, fever, immune compromise, or psychological distress [1]. While the relationship between the virus and the stress response is clear at the level of the organism, how latent HSV interfaces with the cellular environment to initiate reactivation at the molecular level remains obscure. What is becoming clear is that cell survival pathways are involved in the induction of reactivation, and that transition of the HSV genome from latency to transcriptional activity and replication is the sum of several contributing factors.

1.3.2.1 Cellular events leading to HSV reactivation:

Clues to cellular pathways that enable the exit of HSV from latency have come from agents that induce reactivation in an experimental setting. NGF withdrawal, neuronal explant, transient heat shock, and treatment with histone deacetylase (HDAC) inhibitors are some of the classical methods by which reactivation has been stimulated from experimental HSV latency [1]. The success of these treatments in inducing reactivation points to stress response and cell survival pathways as being influential in provoking the latent virus to reactivate.

The most well defined cellular mechanism that stimulates HSV reactivation is induced by withdrawal of NGF from latently infected neurons [46]. Removal of NGF shuts off signaling through the TrkA receptor and leads to inhibition of Akt activity (Figure 1.2), an event sufficient to induce reactivation [47]. Farther downstream in the response to NGF deprivation is the induction of the caspase cascade [52], which has also been indicated as a key regulatory point in effecting HSV reactivation [53] (Figure 1.2). Less is known about the mechanisms involved in stimulating reactivation via other methods, such as heat shock, partly due to the global changes involved in enacting the stress response [54]. In the case of a response involving vast transcriptional changes it is conceivable that the HSV lytic program becomes active alongside upregulated cellular genes. This idea is consistent with the observation that histones associated with the lytic viral promoters accumulate marks of activated transcription following exposure to reactivation stimuli [55, 56]. Additionally, suppression or loss of the pro-latency influence of the immune system could contribute to successful reactivation through alleviating repression of the virus [57]. The scope of cellular processes that enable HSV reactivation has not been defined beyond this rudimentary understanding however, and the contribution of these pathways to human recrudescent disease is not yet clear.

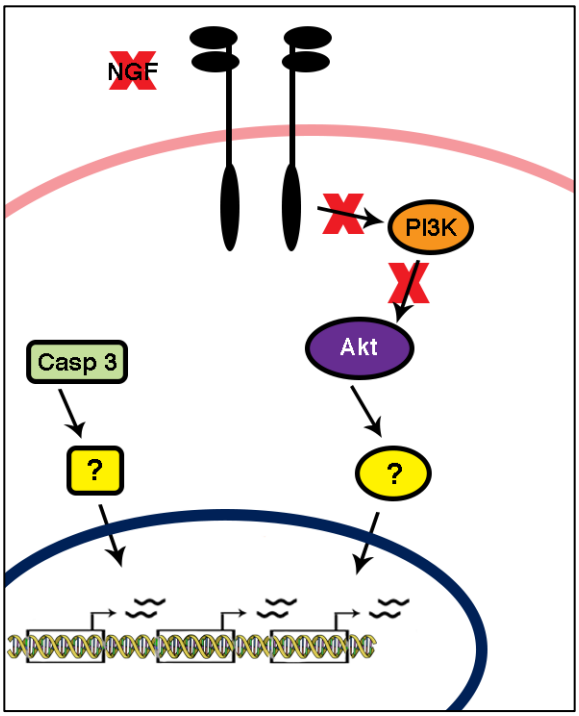

Figure 1.2 Cellular pathways leading to HSV reactivation
HSV reactivation is induced by removal of NGF. In the absence of NGF the receptor tyrosine kinase TrkA does not dimerize and PI3K activation does not occur. Owing to PI3K shutoff, Akt is inactive. Disruption of TrkA, PI3K or Akt activity is sufficient to induce reactivation [47], however downstream effectors linking this pathway to the HSV genome have not yet been elucidated. It has been demonstrated that caspase 3 activation in response to NGF deprivation is necessary for efficient HSV reactivation [53], however the relationship of caspase 3 activation to other cellular signaling pathways in this instance is not yet clear.

Following exposure to stress stimuli, certain physiological changes in the neuron take place that may favour successful viral reactivation. One such event is the relocalization of HCF to the nucleus in response to stress [58], where it further localizes to the HSV IE promoters [59]. HCF is known to recruit chromatin remodeling machinery to remove repressive histone marks from the HSV genome [60], and this interaction may be important for reactivation to proceed. Oct-1 induction has been reported following exposure to noxious stimuli [61], providing a potential means of overcoming low levels of this cofactor in the neuron. Collectively these reports demonstrate a stress-dependent reorganization of the theorized barriers to initiating lytic replication in the neuron nucleus, resulting in an environment more permissive to the productive cycle.

1.3.2.2 Viral response to reactivation stimuli:

Two contemporary theories have arisen on how latent HSV navigates the transition from latency to transcriptional activity and replication. One theory posits that the cellular stress response induces transcription from all responsive viral genes, generating a pool of viral proteins that mediate lytic cycle re-entry [62]. Central to this theory is the idea that in reactivation the lytic replicative cycle is restarted at the point of IE gene induction. This is supported by the observation that, following reactivation stimuli, transcription from all temporal gene classes proceeds in the absence of viral protein synthesis [62, 63]. The finding that several viral promoters are induced by the stress response is also consistent with concurrent induction of lytic genes by cellular factors [64]. An alternate theory posits that VP16 expression is specifically induced by the cellular stress response and that this event initiates exit from latency [65]. Support for this theory comes from the observation that in the absence of a functional VP16 activation domain reactivation does not proceed past VP16 promoter induction [65]. To unite the results supporting these two theories, a model has been proposed wherein the cellular stress response elicits an "animation" phase from the virus [63]. During animation, repression is alleviated and HSV mRNA is synthesized from all gene classes without adherence to the lytic expression cascade [63]. This may be followed by a second phase, with progression being determined by factors such as the intensity of the stress response versus availability of mechanisms that can return the animated virus to a repressed state. In the second phase, factors required for activation of the IE genes by the VIC become available in the nucleus [63], and the majority of latent HSV genomes will progress to productive infection.

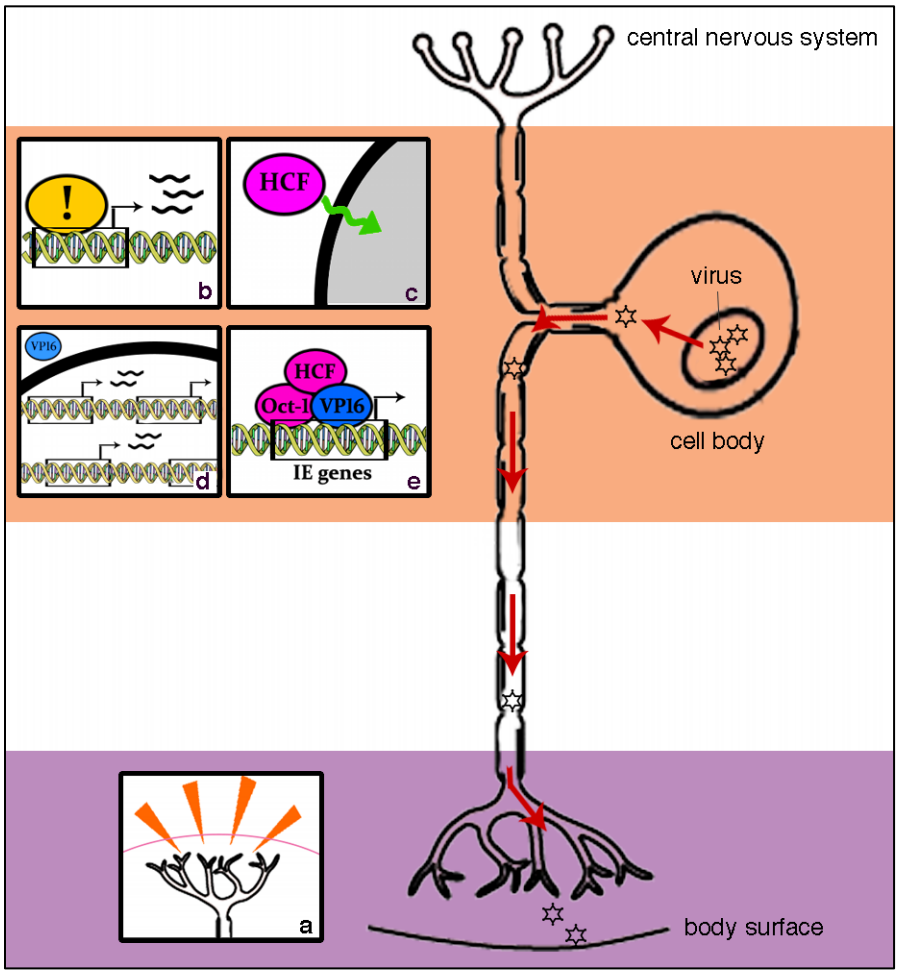

Figure 1.3. Factors governing HSV reactivation from latency.
HSV reactivation in latently infected neurons occurs in response to stress. a) the process of reactivation is provoked by the experience of stress by the host. Exit from latency is coordinated by several molecular events: b) cellular stress response effectors induce transcription from the latent HSV genome. c) physiological changes, such as the relocalization of HCF to the nucleus, overcome barriers to initiating productive infection. d) the virus undergoes an animation phase, where transcription occurs without requirement for prior viral protein synthesis and VP16 is manufactured. d) the lytic gene expression cascade is re-entered at the point of VIC initiation of immediate early genes. Image credits: neuron adapted from [26], nucleosomes adapted from [27].

1.4 Models of HSV latency

A common thread in HSV latency research is that the type of model employed influences how experimental results are interpreted. There exists a question of which experimental latency scenarios can be considered relevant to human HSV infection, and this interferes with determining parts of the latency-reactivation cycle that may be vulnerable to intervention or useful as a platform for other therapies. Studying HSV

reactivation in the human neuron has been possible only in limited circumstances—such as human ganglia obtained at autopsy—and as such, a reasonable facsimile of the neuronal environment in which to study the virus has been long sought. Current approaches for the study of HSV latency utilize small animal models, cultures of extracted primary neurons or neurons derived from pluripotent cells, cell culture models, or some variation thereof.

1.4.1.1 Small animal models:

With certain limitations HSV latency can be modeled in laboratory animals, with the bulk of this research being performed in the mouse. The benefit of utilizing small animal models lies in the ability to simulate the natural course of HSV infection, with lytic infection at the body surface feeding establishment of a latent reservoir in the TG. However, issues of host restriction [66] and the inherently complex nature of studying molecular events in an animal model complicate this approach. The latency-reactivation cycle is specifically adapted to human neurons, and as infection in the mouse model does not follow the same course as in humans, the resemblance of HSV latency between the two species has been questioned (reviewed in [67]). The course of HSV infection in the rabbit model more closely approximates human disease, including features such as spontaneous viral shedding that are absent from HSV pathogenesis in the mouse [67]. While the number of studies is relatively small, HSV latency research performed in rabbits has challenged findings from the mouse model—for example the converse finding that in rabbits the LAT facilitates transcriptional permissiveness of the lytic genes [68]. Small animal models are generally not well-suited to molecular studies owing to limitations in manipulation and sensitivity. Isolating events contributing to HSV latency and reactivation in infected animals has therefore relied on elegant experimental design. The use of viral recombinants which mark infected neurons according to promoter activation [65, 69], and the use of techniques to distinguish reactivating neurons in whole ganglia [70] have been able to overcome some of these limitations.

1.4.1.2 Models utilizing primary neurons:

Methods using cultured primary neurons have also been developed to probe the mechanisms of HSV latency and reactivation. The oldest of these methods involves neuronal explant, in which ganglia of latently infected animals are excised and cultured

[71]. The benefit of this method is that explanted neurons can be manipulated in isolation from the animal, however the stress experienced by the cells during this procedure induces major physiological changes that would not be present during natural reactivation [72]. A modification of the explant approach is to extract and dissociate primary neurons prior to infection with HSV [73]. This allows for better control of the infection and reactivation process, and has been an important tool for deciphering virus-cell interactions. This method remains limited by the issue of host restriction, however, and inhibition of viral replication (achieved by the use of antiviral drugs or viral mutants) is a prerequisite for latency establishment. In an eloquent variation, animal neurons grown in dual chamber systems separating the axon from cell body have been used to recover the contributions of viral entry at the axon terminus [51]. This chambered system obviates the need for replication inhibition, and is a powerful tool for studying the latency-reactivation cycle.

1.4.1.3 Cell culture models:

Owing to their ease of use, a variety of cultured cell models have been developed to host experimental HSV latency—termed "quiescent infection" in the context of cell culture. The best described system utilizes PC-12 cells, a rat pheochromocytoma cell line that can be induced to develop a neuronal morphology by incubation with NGF [74]. The method of establishing latent infection in differentiated PC-12 cells is similar to that of primary neuron cultures, where viral replication inhibition is required to develop a pool of quiescently infected cells suitable for reactivation studies [74]. This approach of stimulating neuronal differentiation from a precursor cell has been attempted with the human NT2 teratocarcinoma cell line [75], the human SH-SY5Y neuroblastoma cell line [76], and most recently by using induced pluripotent stem cells (iPS) of human origin [77], however use of these differentiated cells as models of HSV latency has not been well characterized. To capture the mechanisms of viral repression at work in untransformed cells, quiescent infection in non-neuronal human cells has also been explored, as in the case of normal human diploid fibroblasts [78].

1.4.1.4 Viral mutants in HSV latency models:

Many studies seeking to decipher the HSV latency-reactivation cycle have relied on the use of viral mutants, either to promote entrance into latency by artificially suppressing

the lytic cycle or to determine the contribution of particular genes to HSV reactivation. The major viral trans-activating proteins ICP0, ICP4, and VP16 have most commonly been altered to facilitate development of a non-productive infection [79-82], and provided exogenously to stimulate reactivation [83, 84]. VP16 and ICP4 perform essential functions in production of infectious progeny [85, 86], and deletion of either gene severely decreases the likelihood that the virus will progress through lytic replication. Functional VP16 is essential during virion assembly and egress, however, specific disruption of the C-terminal activation domain has permitted isolation of the contributions of VP16 to IE gene transcription [87]. VP16 activation domain mutants have facilitated studies indicating the importance of this region in reactivation [65], particularly in response to stress [88]. ICP0-null mutants are frequently used in studies probing the effects of cellular antiviral mechanisms, as the absence of this protein exposes the viral genome to cell-mediated repression at low multiplicities of infection [89]. While ICP0 is not essential for exiting latency, it is required for production of progeny virion [90] and can provoke even tightly repressed genomes to re-enter the lytic cycle [78]. The use of viral mutants has been invaluable to unraveling the HSV latency-reactivation cycle within the model systems described by specifically identifying functional regions of the virus involved in each stage of its life cycle.

1.4.1.5 Contributions:

Collectively, the various models used to unravel the mechanics of HSV latency and reactivation have generated a framework of how infection is expected to occur in a human host. Contributions from small animal models have yielded a broad understanding of factors involved in the latency-reactivation cycle, while *in vitro* models have isolated the cellular and viral mechanisms at work. No model perfectly recapitulates the human neuron, although several animal models have been developed that are able to approximate this environment for the virus. With the majority of available models being derived from animals, there is both a need to confirm findings from these models within a human context and investigate the role of human neuron-specific factors. To address this need, human cell lines established from neuronal precursor cells—in a manner similar to the differentiated

PC-12 cell model—may prove useful by linking the human and neuronal requirements of the virus.

1.5 Medulloblastomas

Medulloblastomas are malignant primary central nervous system tumours diagnosed most often in children. They are a heterogeneous class of tumours thought to arise from various derangements in the developmental program of the cerebellum. Current theory on the carcinogenesis of medulloblastomas posits that proliferating neural progenitor cells suffer a deregulation of pathways crucial for normal transition into differentiated cells, and this allows for aberrant expansion of the cell population (reviewed in [91, 92]). Several subclasses of medulloblastoma exist, with inappropriate activation of Shh and Wnt pathways known to drive formation of these tumours [93, 94].

Medulloblastoma cell lines are known to develop the characteristics of neuronal or glial cells when exposed to differentiating agents [95, 96], although the capacity for differentiation varies with cell line and treatment [97]. Differentiation is typically characterized by the presence or absence of proteins specific to cells of either neuronal or glial lineage. There has been little investigation to define the differentiated medulloblastoma cell and its usefulness as a model, in contrast to the wealth of studies performed on other nervous system tumour cell lines (such as the SH-SY5Y neuroblastoma cell line) in both differentiated and undifferentiated states [98, 99].

Chapter 2 Rationale and objectives

The purpose of this project was to determine if medulloblastoma cell lines could be induced to differentiate into cells that provide an environment suitable for investigation of HSV latency and reactivation. To this end, the first aim was to characterize differentiation of medulloblastoma lines as neuronal or glial. The second aim was to determine if latent HSV infection of these differentiated cells could be achieved, and what parameters were necessary for this to occur. Finally, the process of HSV reactivation was examined within the differentiated medulloblastoma cell lines.

Chapter 3 Materials and Methods

3.1 Cell culture

Three human medulloblastoma cell lines were utilized in this study: ONS-76 and UW228, obtained from Dr. Michael Taylor (The Hospital for Sick Children, University of Toronto), and Med283, obtained from the American Type Culture Collection. To support analysis of these cell lines, the Vero line of African Green Monkey kidney cells, U2OS line of human osteosarcoma cells, PC-12 line of rat pheochromocytoma cells, and MRC-5 line of human fetal fibroblasts were also used. Immunofluorescent staining experiments additionally utilized cultures of neurons harvested from dorsal root ganglia of adult male Wistar rats, prepared by Zhengxin Ying (Cameco MS Neuroscience Research Center, University of Saskatchewan).

All cell cultures were maintained in a 37°C, 5% CO_2 incubator (culturing conditions) throughout the course of experimentation unless otherwise indicated. Complete media formulations used for each cell line are listed in Table 3.1, and all media used in the course of study additionally contained 1% penicillin and streptomycin (Life Technologies) to prevent bacterial growth. When confluent, adherent cell lines were reseeded by incubating with trypsin-EDTA (Life Technologies) followed by dilution in appropriate media and transfer to a new 75cm^2 culture flask. Non-adherent cell lines were diluted in appropriate media and transferred to a new culture flask without trypsin-EDTA incubation.

3.2 Virus

The herpes simplex virus type 1 strain KOS was utilized as the wild type strain in all experiments. The KOS-derived HSV mutant V422 lacks the C-terminal activation domain of VP16 [100] and was obtained from Dr. James Smiley (University of Alberta). The HSV n212 mutant, utilized in Gardella gel experiments, is similarly derived from strain KOS and lacks ICP0 activity by virtue of a nonsense mutation inserted into both copies of the gene [101]. The n212 mutant was also obtained from Dr. James Smiley (University of Alberta).

Table 3.1 Cell lines and complete growth media used

Cell line	Complete media composition
Med283	MEM, 10% FBS, 1mM Na pyruvate, non-essential amino acids
MRC-5	D-MEM, 10% FBS
ONS-76	D-MEM, 10% FBS
PC-12	RPMI 1640, 10% inactivated horse serum, 5% FBS, 2mM L-glutamine
U2OS	D-MEM, 10% FBS
UW228	D-MEM/F12 mix, 10% FBS
Vero	D-MEM, 10% NBCS
MEM; minimal essential media, FBS; fetal bovine serum, D-MEM; Dulbecco's modified Eagle medium, RPMI; Roswell Park Memorial Institute medium, F12; Ham's F12 nutrient mixture, NBCS; newborn calf serum. Low serum media contains the same composition with serum content reduced to 1%. All listed reagents were obtained through Life Technologies.	

Infection by all HSV strains was performed as follows. Virus stock was diluted to the indicated multiplicity of infection (MOI, plaque forming units per cell) in D-MEM for a final volume of 250μl per individual 9.5cm^2 well of a 6-well plate. MOI was calculated using an estimate of 1x10^6 cells per 9.5cm^2 well if cells were confluent, and by averaging cell density calculated from 3 independent microscope fields if cells were not confluent. Cell cultures were prepared for inoculation by removing media and rinsing with sterile phosphate buffered saline (PBS). Inoculum was then added and cultures incubated in culturing conditions for 1 hour with gentle rocking every 10 minutes. After incubation, the inoculum was removed and wells were washed with 2ml of pH 3.0 glycine-saline buffer followed immediately by two PBS washes. The appropriate culturing media (Table 3.1) was then added and the plate returned to the incubator. When necessary, acyclovir (ACV, Sigma) was added to cultures at a concentration of 100μM 24 hours before infection.

HSV KOS stocks were created previously in this laboratory by amplifying the virus and determining stock titer on Vero cells. HSV V422 and n212 possess deletions that significantly impair viral replication in many cell lines, and stocks are best grown in U2OS cells, which complement these defects and permit high titers to be obtained [87, 102]. Stocks of the two mutant viruses were generated by infecting culture flasks of confluent

U2OS cells at an MOI of 0.05 (with input virus diluted to 6ml/flask to accommodate the large surface area), followed by incubation in complete media containing 3mM hexamethylene bis(acetamide) (HMBA, Sigma) to aid plaquing efficiency. Virus was harvested when the majority of infected cells displayed cytopathic effects (CPE), characterized as cells becoming large, rounded, and refractile. Purification of viral stocks consisted of pelleting infected cultures, lysing cells through a series of three freeze-thaw cycles, and centrifugation to clear cellular debris.

Adenovirus vectors were constructed previously in this laboratory to express the human CREB3/Luman protein (Luman), or *Escherichia coli* β-galactosidase (LacZ). To infect cell cultures, growth media was removed and replaced with the appropriate adenovirus vector diluted to an MOI of 100 in a final volume of 250μl per 9.5cm^2 well in OptiMEM (Life Technologies). The virus was incubated with the cells for 1 hour in culturing conditions with rocking every 10 minutes, following which the inoculum was replaced with 2ml of media appropriate for the infected cells (Table 3.1).

3.3 Plaque Assay

Plaque assays were utilized to determine the titer of infectious virus present in a given sample. For analysis of all HSV strains, U2OS cells were plated at a density of 1x10^5 cells per well in 24-well plates 24 to 48 hours prior to infection. Samples were subjected to three freeze-thaw cycles followed by centrifugation for 10 minutes at 100*g*, and the resulting supernatant was used to prepare serial dilutions in D-MEM. Tenfold dilutions from 1x10^{-2} to 1x10^{-7} were prepared and tested in the plaque assay. Media was removed from the U2OS cells and 100μl of diluted sample was added to each well, followed by 1 hour of incubation with rocking every 10 minutes. At 1 hour post infection, inoculum was removed and D-MEM containing 1% pooled human serum (Fisher Scientific) and 3mM HMBA was added. When plaques developed to a visually apparent size, the U2OS cells were fixed in ice-cold methanol for 15 minutes, and stained with Giemsa stain (prepared by GMP at the Western College of Veterinary Medicine) to aid visualization. Wells containing between 1 and 50 plaques were counted and divided by the dilution factor to determine the number of plaque forming units (pfu) per ml.

3.4 WST assay

The WST-1 assay (Roche Applied Science) was utilized to determine proliferation of cells in culture. 96-well plates were seeded with 100μl of $1x10^5$ cells/ml for a final concentration of $1x10^4$ cells/well. Media was replaced every 3 days to support long-term cell growth. To perform the assay, 10μl of WST-1 reagent was added to each well and the plate incubated in culturing conditions for 45 minutes. After incubation, absorbance at 450 nanometers was read in a VMax Kinetic ELISA Microplate Reader (Molecular Devices). The WST-1 reagent is a tetrazolium salt cleaved to produce a formazan dye through a mechanism dependent on active cellular metabolism, therefore the quantity of dye produced directly correlates to the number of metabolically active cells in culture.

3.5 Indirect immunofluorescent staining

Indirect immunofluorescent staining (IF) was utilized to determine the presence of proteins in a cell, as assessed by fluorescent emission from specific bound antibody complexes. To promote adherence of differentiating cells, coverslips were soaked in concentrated HCl, washed thoroughly with ultrapure water, soaked in ethanol, and finally coated with a solution of 40μg/ml poly-D-lysine (Sigma) and 4μg/ml laminin (BD Biosciences). Cells were seeded into 6-well plates containing prepared coverslips at an initial density of $2x10^4$ cells per well and grown as indicated in experiment details. PC-12 cells were differentiated through incubation with 100ng/ml NGF (Cedarlane) for 4 days. Cells were prepared for staining by fixation in ice-cold methanol for 20 minutes at -20°C. Fixed cells were stained according to the standard protocols of the Misra laboratory (M protocol) or Verge laboratory (VV protocol), as per the location of the staining.

The M protocol was utilized for ONS-76, UW228, and PC-12 cells, and was performed as follows: fixed cells were incubated in 2ml/well of blocking solution, comprised of 10% NBCS and 0.1% Tween 20 (USB Products) in PBS, for 20 minutes at room temperature. Blocking solution was removed and 30μl of primary antibody, diluted by the factor indicated in Table 3.2, added directly to each coverslip. Plates with primary antibody were incubated for 30 minutes in a moist chamber to prevent drying. Following incubation wells were washed 4 times with PBS and incubated for 5 minutes in blocking solution. Fluor-conjugated secondary antibody was diluted by the factor indicated in Table

3.2, and 30μl added to each coverslip. Plates were then incubated for 30 minutes in a dark moist chamber, following which wells were washed an additional 4 times with PBS to complete the staining procedure.

Table 3.2 Reagents used in IF staining

Antibody	Source	Dilution
Primary antibodies		
β-tubulin III	Millipore, MAB1637	1:50
Brn3A	Sigma B9684	1:100
GFAP	DAKO, Z0334	1:100
NF (M protocol)	Sigma N5264	1:50
NF (VV protocol)	Abcam, ab8135	1:100
NeuN	Abcam, ab104225	1:50
TrkA	Biovision, 3194-100	1:50
Secondary antibodies		
Alexa 488	Molecular probes, A-11001	1:500
Alexa 546	Molecular probes, A-11010	1:500
Nuclear stains		
PI	Molecular probes, P1304MP	1μg/ml
DAPI	--	In mounting media
Brn3A; brain-specific homeobox/POU domain protein 3A, GFAP; glial fibrillary acidic protein, NF; neurofilament, NeuN; neuronal nuclear antigen (Fox-3), TrkA; neurotrophic tyrosine kinase receptor type 1, PI; propidium iodide, DAPI; 4'6-diamidino-2-phenylindole. Secondary antibodies are fluor-conjugated anti-mouse or anti-rabbit immunoglobulin. Antibodies were diluted in blocking solution for the M protocol and in PBST for the VV protocol. Nuclear stains were diluted in ultrapure water.		

The VV protocol was utilized for UW228 cells and rat neuron cultures and was performed as follows: blocking solution, comprised of 2% horse serum, 2% goat serum, and 0.5% bovine serum albumin in phosphate buffered saline + 0.1% Triton-X (PBST), was added to fixed cells and incubated for 30 minutes. This was then removed and 100μl of diluted primary antibody (Table 3.2) added to each coverslip. Primary antibody incubation took place overnight at 4°C, and unbound antibody was washed off the following day with 3 PBST washes of 5 minutes each. 100μl of secondary antibody dilution was added to the coverslips, and plates incubated for 1 hour in the dark. The coverslips were again washed three times with PBST for 5 minutes to complete the staining procedure. Staining using the VV protocol took place at the Cameco MS Neuroscience Research Center, with all reagents excepting antibodies graciously provided by Dr. Valerie Verge.

For both protocols, slides were prepared for visualization by inverting coverslips onto a drop of mounting media (50% PBS/50% glycerol, commercial preparation containing DAPI used for the VV protocol) and sealing with clear nail polish. Cells were examined by fluorescent microscopy using an Olympus BX51 microscope, and images captured and edited using DP Controller (Olympus) and Northern Eclipse software (EMPIX Imaging Inc.).

3.6 RNA purification and qRT-PCR

To determine and quantify transcription from specific cellular and viral genes, quantitative real-time polymerase chain reaction (qRT-PCR) was performed on RNA extracted from culture samples. For isolation of total RNA from samples, the RNeasy Plus Mini kit (Qiagen) and included procedure for mRNA extraction were used. Purified RNA was quantified on a Nanodrop 2000c spectrophotometer (Thermo Scientific) and a standardized amount of RNA (to a maximum of 1μg) was used as template for cDNA synthesis. The Quantitect Reverse Transcription kit (Qiagen) and a PTC-200 Peltier Thermal Cycler (MJ Research) were utilized to generate cDNA for use in qRT-PCR according to the protocol specified by the manufacturer.

PCR reactions were set up in duplicate using the Brilliant II SYBR Green qPCR Master Mix kit (Agilent Technologies), and the abundance of specific gene transcripts quantified by qRT-PCR in a Stratagene Mx3005P thermal cycler. The thermal program

consisted of heating to 95°C for 10 minutes, followed by 40 cycles of 95°C for 30 seconds, 55°C for 1 minute, and 72°C for 1 minute, and finally one cycle of 95°C for 1 minute, 55°C for 30 seconds, and 95°C for 30 seconds. Ct values generated through this program were converted to absolute values using standard curves correlating Ct and the number of gene equivalents present. Standard curves were produced by performing PCR on serial dilutions of purified HSV or HeLa cell DNA and generating the equation of the line of best fit. PCR primer targets and sequences are listed in Table 3.3.

Table 3.3 Primers used in qRT-PCR reactions

Primer target	Source	Sequence
GAPDH	Valderrama *et al.* [103]	F – TGCCTCCTGCACCACCAACTGC
		R – GGGCCATCCACAGTCTTCTGGG
HSV ICP0	In-house	F – CTCCTCTGCCTCTTCCTCCT
		R – TTGTTCACGTAAGGCGACAG
HSV LAT	Du *et al.* [62]	F – GCATAGAGAGCCAGGCACAAAA
		R – ACGTACTCCAAGAAGGCATGTG
HSV TK	In-house	F – CCATCAACACGCGTCTGCGTT
		R – CCAGTAAGTCATCGGCTCGG
HSV VP5	In-house	F – CTTCTGCGAGACGAGCTTTT
		R – CCACTTTCAGGAAGGACTGC
HSV VP16 (for KOS)	In-house	F – GGACGAGCTCCACTTAGACG
		R – AGGGCATCGGTAAACATCTG
HSV VP16 (for V422)	K. Schroeder	F – GCAGGCCCTCGATGGTAGAC
		R – CCGCGCCTCTGGGTACTTTA
HVEM	K. Schroeder	F – CCAAGTGCAGTCCAGGTTATCG
		R – TTGCTTAGGCCATTGAGGTGG
Nectin-1	Vetter *et al.* [104]	F – ACCAACCCCATCGGTACAC
		R – GGGGTGTAGGGGAATTCTGT
ZF	In-house	F – CCGGGATCCATGAGGCATAGCCTG
		R - CCGCTCGAGAGAGCAGATTACTTGA

3.7 DNA purification and analysis

To determine the number of viral and cellular genome copies present in a sample, total DNA was purified and assessed by qRT-PCR. Isolation of total DNA from infected cultures was performed using the DNeasy Blood and Tissue kit (Qiagen) and included procedure for extraction from cultured cells. Purified DNA from this procedure was quantified on a Nanodrop spectrophotometer. In each sample the viral gene target VP16 and the cellular gene target ZF (primer sequences in Table 3.3) were quantified by qRT-PCR in a Stratagene Mx3005P thermal cycler, with reactions set up using the Brilliant II SYBR Green qPCR Master Mix kit (Agilent Technologies). Thermal cycling of PCR reactions followed the same program as detailed for qRT-PCR analysis of cDNA (Section 3.6). Ct values were converted to absolute values using standard curves specific to each primer set, and the number of viral targets was divided by the detected cellular targets to provide the number of viral genome copies present per cell. This calculation controlled for variation in the total number of cells present in each well.

3.8 Gardella gels

The Gardella gel protocol has been previously described for use in detecting latent herpesviruses [105, 106] and was adapted for use with infected medulloblastoma cell lines. To create the resolving portion of the gel, 225ml of molten 0.75% low melting point agarose (Life Technologies) in 0.5x tris borate EDTA buffer (TBE) with 20μl of SYBR Safe DNA gel stain (Life Technologies) was first prepared and poured into a 20.25cm x 15cm casting tray with a 15-well comb set 4.5cm from the top of the gel. Once this gel had polymerized, the comb was removed and the top 4.5cm excised and discarded. To create the lysis portion of the gel, 50ml of molten 0.8% agarose (Life Technologies) was prepared and allowed to cool before addition of 2% SDS (prepared by GMP) and 1mg/ml self-digested pronase (Sigma). The comb was replaced into the casting tray and the molten lysis gel poured to replace the excised portion of the resolving gel.

Cells were seeded in a staggered fashion so the appropriate duration of viral infection was reached on the day the Gardella gel was loaded. As the lysis gel was polymerizing approximately $5x10^5$ cells for each indicated time point were rinsed with PBS and scraped into 15ml Falcon tubes, followed by 4°C centrifugation at 200*g* for 10 minutes.

The supernatant was discarded and cells gently resuspended in 25μl of Gardella sample buffer (20% Ficoll (Pharmacia), 0.01% bromophenol blue (EMD) in TBE) and kept on ice until gel loading.

At 4°C the polymerized gel was immersed in 0.5x TBE and loaded with 25μl of cell sample per well. To lyse the loaded cells the gel was run first at 40V for 2 hours, followed by resolving DNA from the lysed cells by running the gel for 16 hours at 140V. After running, each lane was cut into 0.5cm slices using a separate scalpel blade for each region within each sample so as to avoid cross-contamination. Gel slices were collected in 1.5ml microcentrifuge tubes and stored at 4°C.

To determine if viral DNA was present, tubes containing gel slices were heated to 65°C for 15-20 minutes to melt the agarose, and 5μl from the resulting liquid was added to PCR reactions as template. PCR reactions were prepared using the TopTaq DNA Polymerase kit (Qiagen). For each 50μl reaction, 5μl of 10x PCR buffer, 0.25μl of TopTaq (both included in the kit), 2μl of both 5μM VP5 primers, 1μl of dNTP mix (Life Technologies), 34.75μl ultra-pure water, and gel template were combined and run in a PTC-200 Peltier Thermal Cycler (MJ Research). The amplification program utilized was 94°C for 3 minutes, followed by 30 cycles of 94°C for 30s, 55°C for 45s, 72°C for 1 minute, and a final extension time of 10 minutes at 72°C. PCR products were run on an 0.8% agarose gel containing 1mg/ml ethidium bromide and visualized on an Alpha Innotech Alpha Imager.

Chapter 4 Results

4.1 Generating neuronally-differentiated medulloblastoma cell cultures

The first aim of this project was to develop human medulloblastoma tumour cell lines into neuronally-differentiated cultures. This was accomplished by screening a variety of known differentiation agents for the ability to stimulate a change in the medulloblastoma cell lines. Differentiated cells identified through the screening process were then examined to determine cell character.

4.1.1 Screen of medulloblastoma cell response to differentiation stimuli

Medulloblastoma cell lines are known to differentiate along a neuronal pathway in response to a variety of chemical agents [95, 96, 107, 108]. A screen of these agents was performed on the Med283, ONS-76, and UW228 medulloblastoma cell lines (Table 4.1) to determine if a population of neuronally differentiated cells could be generated that would be suitable for use in HSV latency studies. Dibutyryl cyclic adenosine monophosphate (DBcAMP) and resveratrol are compounds that have been described to stimulate neuronal differentiation in medulloblastoma cell lines [95, 107]. These agents were therefore screened to characterize their ability to induce differentiation in Med283, ONS-76 and UW228 cells. Because of its role in maintenance of HSV latency, NGF was included in the screen although NGF signaling has been linked to apoptotic pathway induction in medulloblastomas [109]. Aphidicolin has classically been used in neuronal cell culture to control growth of mitotic cells and was also utilized as a screening chemical.
The screen for successful differentiation used three criteria:

i) That the cells developed a neuronal morphology, with features such as the outgrowth of neurite-like processes
ii) That the number of cells in culture became stable, a phenomenon associated with cells becoming post-mitotic
iii) That differentiation be achieved within 15 days of treatment

Table 4.1 Characteristics of medulloblastoma cell lines

	ONS-76	UW228	Med283
Origin	2 year old female	9 year old female	6 year old male
Site	Cerebellum	Posterior fossa	Peritoneum & ascites
Derived	1987	1995	1985
IHC	Neurofilament, enolase, GFAP, S-100 protein	Neurofilament, synaptophysin, GFAP	Neurofilament, enolase, GFAP, S-100 protein
Expression	Neurofilament, enolase	Neurofilament, synaptophysin	Neurofilament, enolase
Source	Tamura *et al.* [110]	Keles *et al.* [111]	Friedman *et al.* [112]

Every possible combination of DBcAMP, resveratrol, NGF and aphidicolin was used to treat an individual culture (Table 4.2), with media being refreshed every 3 days. Morphology was monitored over a 15 day period, and several types were observed to develop by the end of treatment, as summarized in Figure 4.1. Out of the total screened treatments, two cultures of ONS-76 and two of UW228 cells satisfied the criteria and were put forth for further assessment. The treatments resulting in differentiation were DBcAMP and resveratrol with or without NGF for ONS-76 cells, and DBcAMP with or without NGF for UW228 cells. Med283 cells were not stimulated to differentiate according to screen criteria by any of the tested agents or combinations thereof. Table 4.2 lists the morphology developed by each individual treatment group at the end of the screen.

Differentiation of ONS-76 cells in subsequent experiments was achieved through treatment with DBcAMP and resveratrol, and differentiation of UW228 cells with DBcAMP and NGF. The differentiation protocol utilized was as follows: cells were seeded in complete media and allowed to recover for 48 hours before changing to low serum media containing the appropriate differentiation agents. This media was then replenished every three days for the remainder of the experiment, and cells were considered to be differentiated after 12 days of incubation with differentiation agents.

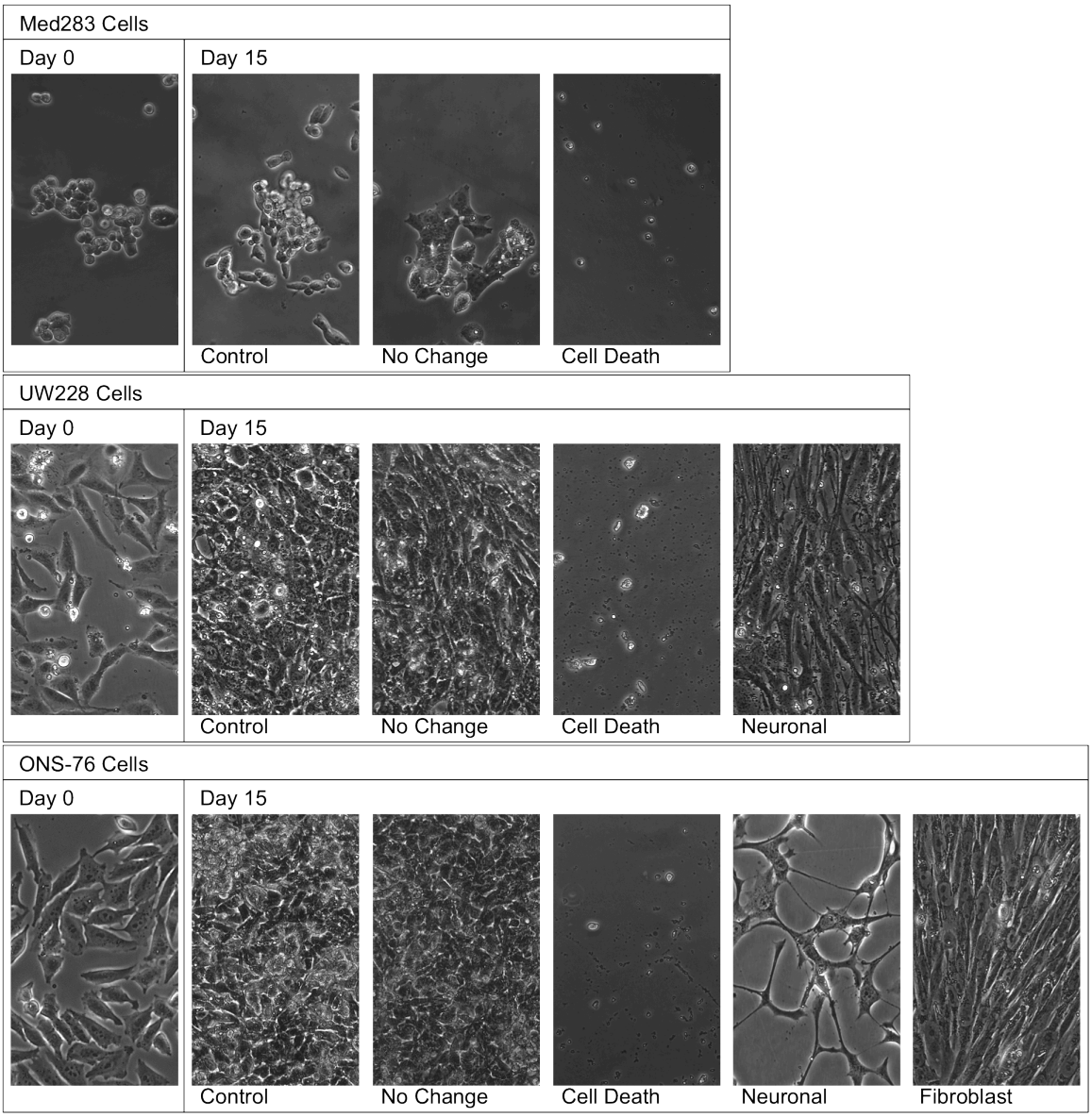

Figure 4.1 Morphology of medulloblastoma cell lines treated with differentiation agents.

Medulloblastoma cell lines Med283, UW228 and ONS-76 were seeded in 24-well plates at a density of $5x10^4$ cells/well in complete media. Cells were allowed to recover for 48h before media was changed to low serum media containing differentiating agents (day 0). Media was replaced every three days, maintaining concentrations of differentiating agents. Pictures are examples of the distinct morphologies developed by treated cultures at day 15. For the morphology developed by individual treatment groups see Table 4.2.

Table 4.2 Morphology of differentiation agent-treated medulloblastoma cell lines

Med283					
Treatment	Morphology	Treatment	Morphology	Treatment	Morphology
D	Death	Media only	No change	RN	Death
R	Death	DR	Death	RA	Death
N	No change	DN	No change	NA	Death
A	Death	DA	Death	RNA	Death
DRN	Death	DNA	Death	DRA	Death
ONS-76					
Treatment	Morphology	Treatment	Morphology	Treatment	Morphology
D	No change	Media only	No change	RN	Fibroblast
R	Fibroblast	DR	Neuronal	RA	Death
N	No change	DN	No change	NA	Fibroblast
A	Fibroblast	DA	No change	RNA	Death
DRN	Neuronal	DNA	No change	DRA	Death
UW228					
Treatment	Morphology	Treatment	Morphology	Treatment	Morphology
D	Neuronal	Media only	No change	RN	Death
R	Death	DR	Death	RA	Death
N	No change	DN	Neuronal	NA	Death
A	Death	DA	Death	RNA	Death
DRN	Death	DNA	Death	DRA	Death
Cultures were seeded and maintained as described in Figure 4.1. Final concentrations of DBcAMP, NGF, resveratrol, and aphidicolin were 1mM, 100ng/ml, 10μM and 4μg/ml, respectively. D; DBcAMP, R; resveratrol, N; NGF, A; aphidicolin.					

4.1.2 Assessment of differentiated medulloblastoma cell proliferation

To characterize changes in proliferation of the differentiating medulloblastoma cells, a WST assay was performed. The growth of differentiating cells was compared to control cells, with the only difference between treatment groups being the presence of differentiation agents. ONS-76 cell cultures treated with DBcAMP and resveratrol do not

proliferate to the same magnitude as untreated controls and instead become relatively stable in number, a phenomenon visually evident by 15 days of differentiation (Figure 4.1). Cessation of growth in differentiating ONS-76 cultures was confirmed by the WST assay, where increases in control cell numbers exceeded that of treated cells (Figure 4.2). UW228 cells also appear to exhibit cessation of growth when treated with differentiating agents (Figure 4.1), and this was confirmed by WST assay results showing relatively stable numbers of differentiating cells in culture (Figure 4.3). As the WST assay correlates cellular metabolic activity to cell number, refreshing growth media may have amplified the oscillations observed in cell proliferation in these results.

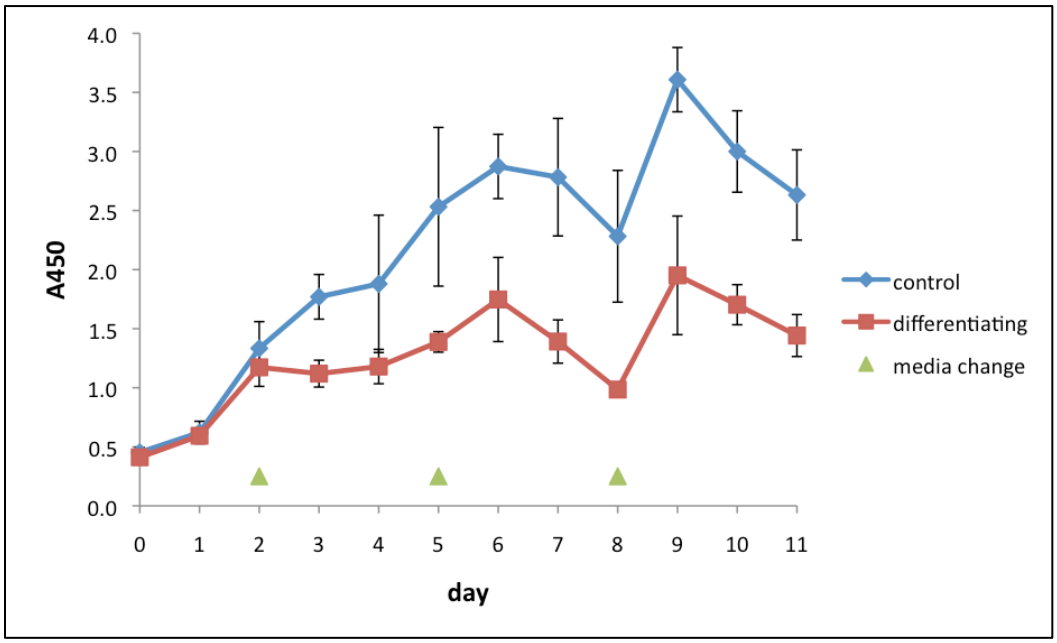

Figure 4.2 Proliferation of differentiating ONS-76 cells.
Proliferation of differentiating and control ONS-76 cells as assessed by a WST assay. Cells were seeded into 12 96-well plates at a density of $1x10^4$ cells/well (day 0) and allowed to recover for 24h before changing media to low serum with or without differentiating agents. At the indicated day, the WST assay was performed on control and differentiating wells in an individual plate as detailed in Methods. Results are an average of 4 replicates. Media was refreshed in all plates on days 2, 5, and 8 (arrowheads).

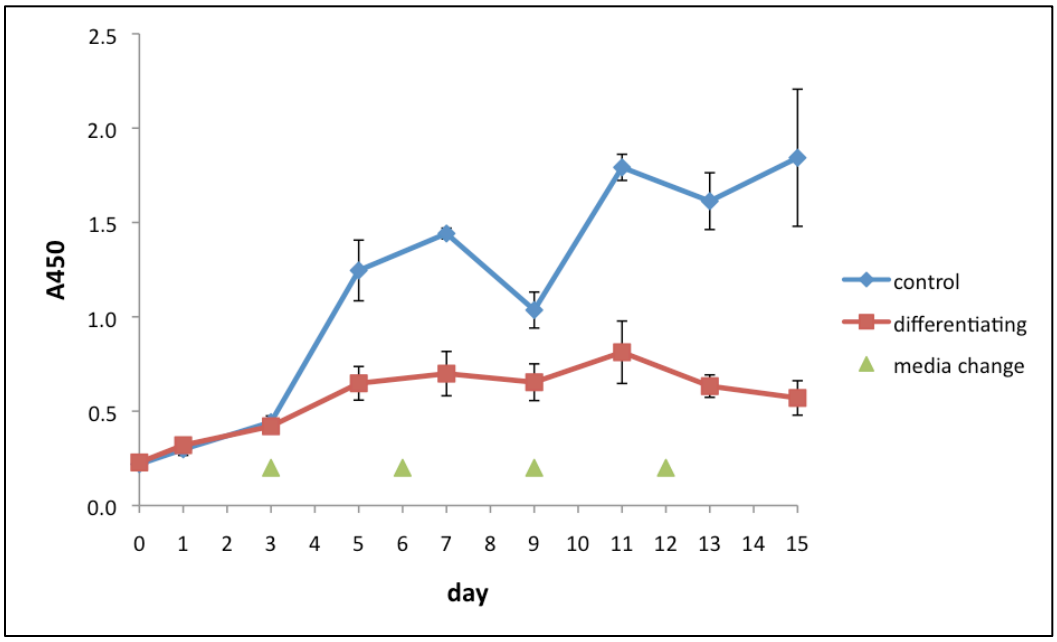

Figure 4.3 Proliferation of differentiating UW228 cells
Proliferation of differentiating and control UW228 cells as assessed by a WST assay. Cells were seeded into 9 96-well plates at a density of $1x10^4$ cells/well (day 0) and allowed to recover for 24h before changing media to low serum with or without differentiating agents. At the indicated day, the WST assay was performed on control and differentiating wells in an individual plate as detailed in Methods. Results are an average of 4 replicates. Media was refreshed in all plates on days 3, 6, 9, and 12 (arrowheads).

4.1.3 Assessment of neuronal protein expression in differentiated medulloblastoma cells

Medulloblastoma cells are thought to derive from immature bipotential cells, and can be induced to develop along glial or neuronal pathways (see Section 1.5). The expression of cell type-specific marker proteins was investigated in differentiating medulloblastoma cells to determine if differentiation correlated with a shift in cell character. To this end, the presence of proteins specific to glia and neurons was defined in UW228 and ONS-76 cells in both states of differentiation. Glial character was assessed by staining cultures for the glial fibrillary acidic protein (GFAP), while neuronal character was determined by staining for class III β-tubulin, brain-specific homeobox/POU domain protein 3A (Brn3A), neuronal nuclear antigen/Fox-3 (NeuN), and neurofilament (NF) proteins. Differentiated PC-12 cells have been widely used as a cell culture model of neurons [113-115], and staining for marker proteins was also performed on these cells. In addition, cultures of primary rat neurons were stained as a positive control for the neuronal marker proteins.

Control ONS-76 cells did not stain for the neuronal proteins NF or β-tubulin, however did stain for the glial marker GFAP as seen in Figure 4.4A. When differentiated ONS-76 cells were stained for these proteins β-tubulin was detected, localizing in projections extending from the cell body (Figure 4.4B). Expression of GFAP in differentiated ONS-76 cells was similar to that of the control cells, and NF protein remained undetectable post-differentiation. Staining of differentiated PC-12 cells revealed the presence of GFAP with localization similar to that of the ONS-76 cells (Figure 4.4C). The presence of β-tubulin was not found, and while NF expression was detected in a few scattered cells it was not seen in the vast majority (Figure 4.4C). These findings appear to contrast with what has been typically documented for expression of GFAP, NF, and β-tubulin in differentiated PC-12 cells [116-118]. Despite the atypical staining of differentiated PC-12 cells in this experiment, it was concluded from the expression of β-tubulin in differentiated ONS-76 cells that treatment with DBcAMP and resveratrol induced differentiation along a neuronal pathway.

Staining performed on control and differentiated UW228 cells using GFAP, β-tubulin, and NF yielded identical results for both differentiation states: the presence of β-tubulin and NF was not detected, and similar levels of GFAP staining were seen in both differentiated and control populations (Figure 4.4D, E). The pool of neuronal targets was expanded to include Brn3A and NeuN, and cultured rat neurons were stained alongside cells as a positive control. UW228 cells in both differentiation states exhibited some staining for NeuN, with a more nuclear localization in differentiated cells and rat neurons than control cells (Figure 4.5). Brn3A staining in differentiated UW228 cells and rat neurons was dispersed throughout the cytoplasm and nucleus, while in control UW228 cells it was detected in a perinuclear cluster (Figure 4.5). Finally, NF staining was performed using an alternate antibody to confirm previous staining results. As shown in both Figure 4.4 (D,E) and Figure 4.5, NF was not detected in the UW228 cells yet intense staining was seen in the processes of the rat neurons. While expression of the tested neuronal and glial proteins did not change upon UW228 cell differentiation, maintained expression of the neuronal proteins Brn3A and NeuN indicated that although treatment did

not induce further neuronal differentiation these cells exhibited a degree of neuronal character.

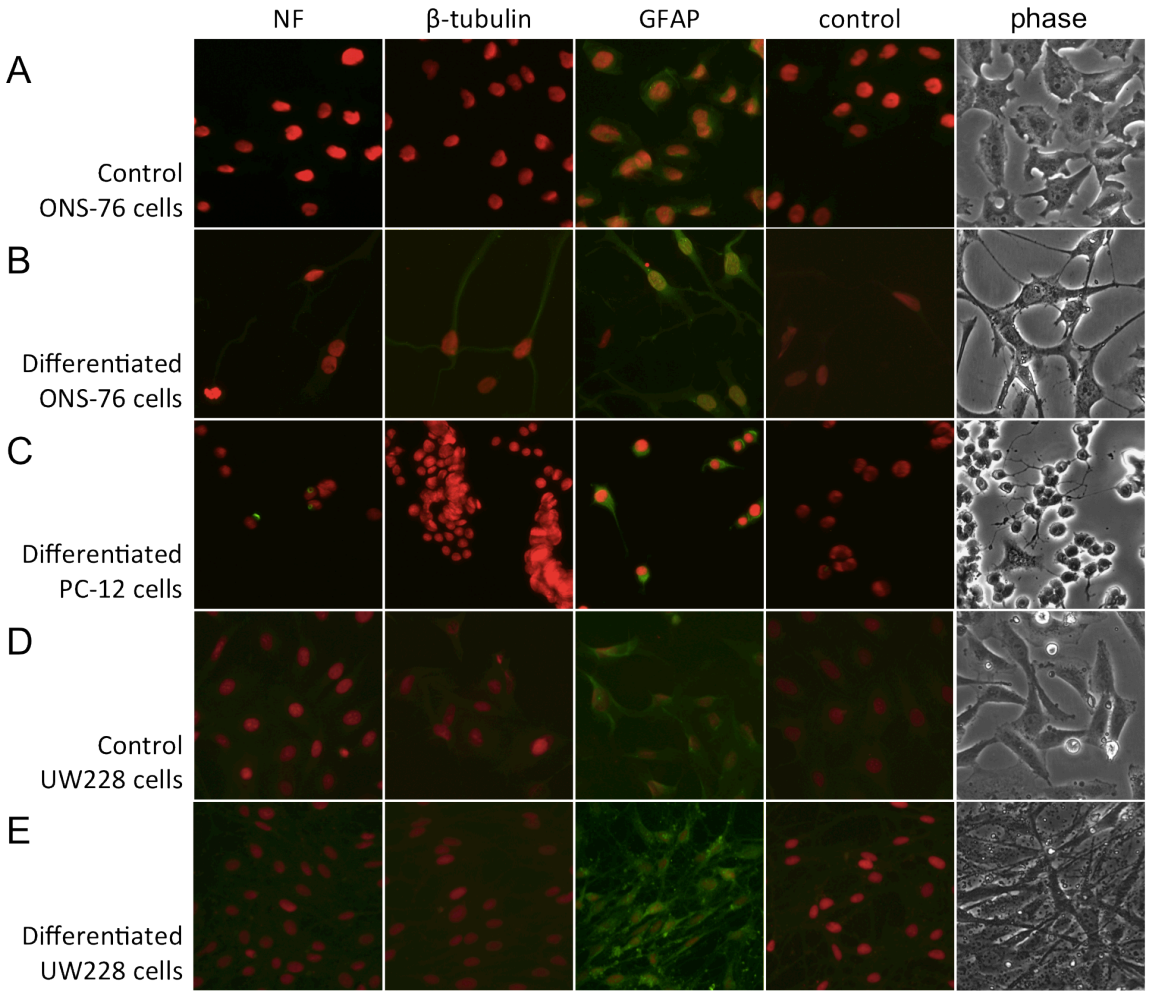

Figure 4.4 Marker protein expression in differentiating medulloblastoma cells
Indirect immunofluorescent staining was performed on the indicated cell populations as per the M protocol detailed in Methods. Cells were grown on coverslips for 2 days for controls and 14 days for differentiated medulloblastoma populations. PC-12 cells were differentiated for 4 days on coverslips before staining. Red nuclear staining is propidium iodide, and green staining results from detection of bound primary antibody. NF; neurofilament, β-tubulin; class III β-tubulin, GFAP; glial fibrillary acidic protein. Control is HSV ICP27 antibody.

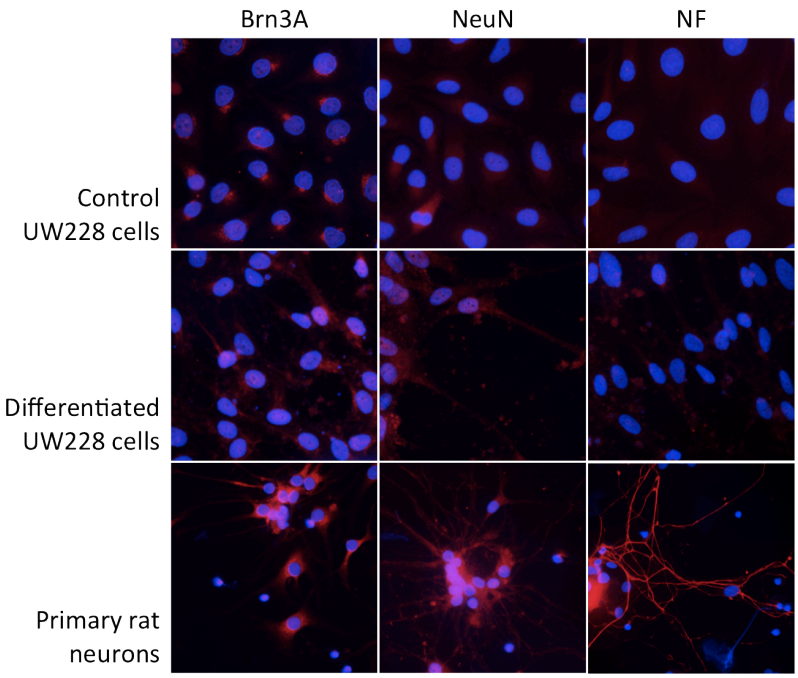

Figure 4.5 Neuronal protein expression in differentiating UW228 cells
Indirect immunofluorescent staining was performed on the indicated cell populations as per the VV protocol detailed in Methods. Control UW228 cells were grown on coverslips for 3 days and differentiated UW228 cells for 14 days. Blue nuclear staining is DAPI and red staining results from detection of bound primary antibody. Rat neuron cultures were prepared on coverslips by Zhengxin Ying.

4.1.4 Expression of herpesvirus entry mediators

It has been demonstrated in other neuronally-differentiated tumour cells that differentiation coincides with changes in expression of proteins which mediate herpesvirus entry [76]. Therefore, expression of the major HSV entry receptors HVEM and nectin-1 was assessed in control and differentiated UW228 cells. HVEM, nectin-1, and GAPDH transcription were determined for differentiated and control cells by qRT-PCR, and fold change in expression was calculated. Results demonstrate no change in nectin-1 expression between differentiation states, and a slight decrease in HVEM expression upon differentiation (Figure 4.6). Ct values obtained for the entry proteins ranged from cycle 20-22, whereas qRT-PCR performed with HeLa genomic DNA (containing the unspliced target genes with introns) returned Ct values of 30-34. This data indicates that transcripts were readily and specifically detected in the UW228 cells, and it was concluded that significant changes in expression of herpesvirus entry mediators were not observed upon differentiation.

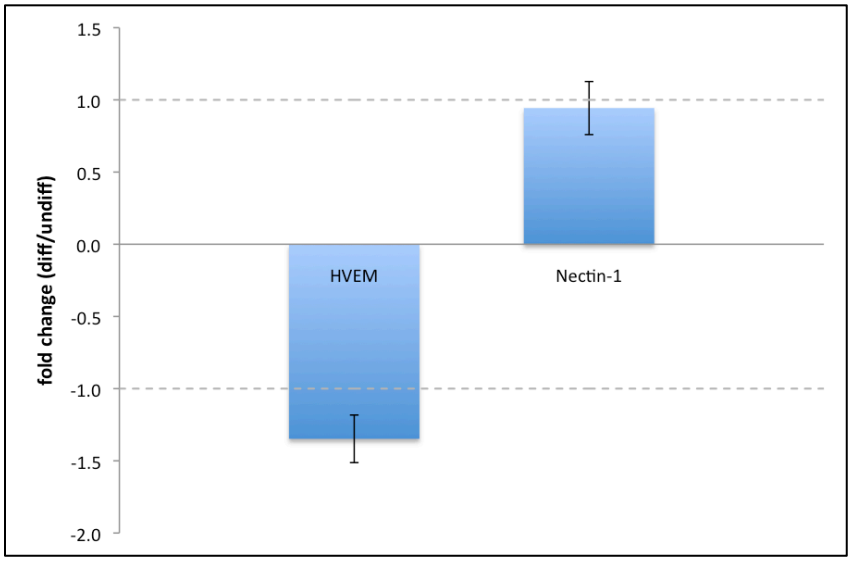

Figure 4.6 Herpesvirus entry protein expression in UW228 cells
Expression of herpesvirus entry mediators HVEM and nectin-1 was assessed by qRT-PCR. Total RNA was extracted from differentiated and control UW228 cells and PCR was performed on cellular targets as detailed in Methods. Expression of HVEM and nectin-1 was normalized to expression of the GAPDH housekeeping gene. Results are an average of two replicates from the same experiment.

4.2 Establishing HSV latency in differentiated medulloblastoma cells

The second aim of this project was to determine if latent HSV infection could be established in differentiated medulloblastoma cells. Various parameters of infection were explored in differentiated ONS-76 and UW228 cells, such as the inhibition of viral replication and use of HSV mutants, to determine requirements for establishing latent infection. Infection was then evaluated to determine if viral latency, defined as the presence of viral DNA in the absence of infectious virus and lytic transcription, had been achieved.

4.2.1 Establishing quiescent HSV infection of differentiated ONS-76 cells

Differentiated ONS-76 cells were assessed for their ability to host latent, or quiescent, HSV infection. To make this determination, the permissivity of ONS-76 cells to HSV replication post-differentiation was evaluated. Differentiated cultures of ONS-76 cells were infected with the wild type HSV strain KOS at an MOI of 1, and viral titer and cellular morphology were tracked over the following 48 hours (Figure 4.7, Figure 4.9). Altered viral strains are often required to overcome the inherent limitations of modeling HSV in cell culture, and as the loss of VP16 during axonal transport has been reported to be important for latency establishment [13] infection with the HSV V422 mutant was also explored. This mutant carries a truncated form of VP16, which lacks the activation domain that initiates entry into the lytic program but remains able to participate in the assembly of functional capsids [100]. Plaque assays were performed to monitor changes in viral titer and demonstrated both KOS and V422 to increase steadily over time (Figure 4.7), a result consistent with replicating virus. In agreement with these results, infected cultures exhibited an increasing number of cells displaying CPE as time progressed (Figure 4.9A). The development of CPE and increase in viral titer occurred more slowly for V422 than KOS, which may be attributable to the impairment of this virus. It was therefore concluded that the environment of differentiated ONS-76 cells did not promote establishment of quiescent infection by HSV KOS or V422, and instead was permissive to productive replication.

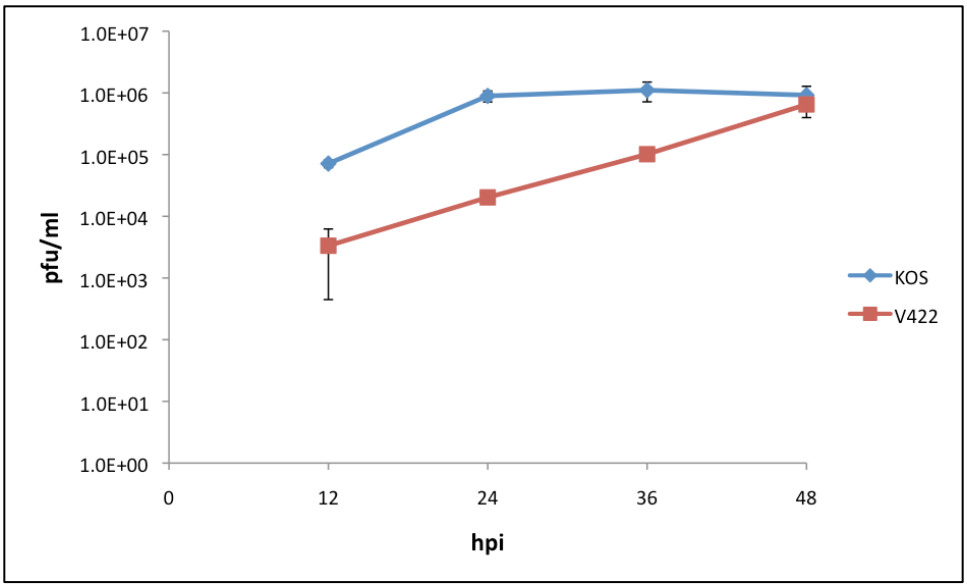

Figure 4.7 HSV replication in differentiated ONS-76 cells
ONS-76 cells were differentiated in 6-well plates and infected with the HSV strain KOS or V422 at an MOI of 1. At the indicated time point, cells were scraped from the well surface and processed for determination of viral titer in a plaque assay (detailed in Methods). Data points are an average of 2 replicates.

Acyclovir (ACV) is an antiviral drug commonly used in treatment of herpesvirus infections, and exerts its activity by terminating viral DNA replication. Cell culture models of HSV latency often rely on ACV to suppress viral replication during the establishment phase [73, 74], therefore it was determined if quiescent infection of differentiated ONS-76 cells could be achieved through use of this chemical. Cultures incubated with ACV were infected with HSV KOS and V422 at an MOI of 1 and viral titer and cellular morphology were again monitored for 48 hours. In the presence of ACV, infectious KOS and V422 were not detectable beyond the first 36 hours of infection (Figure 4.8), a finding consistent with suppressed replication. Despite this result, infected cultures developed CPE similarly to cultures infected in the absence of ACV, with a progressive loss of most cells by 48 hpi (Figure 4.9). V422 titers fell more quickly than that of the wild type and V422-infected cells appeared to survive longer than those infected with KOS, attributable again to the impairment of the mutant, however the overall phenotype was the same for both viruses. As infection with HSV KOS and V422 caused significant toxicity to differentiated ONS-76 cells even in the absence of viral replication, it was concluded that this system was not compatible with hosting HSV latency.

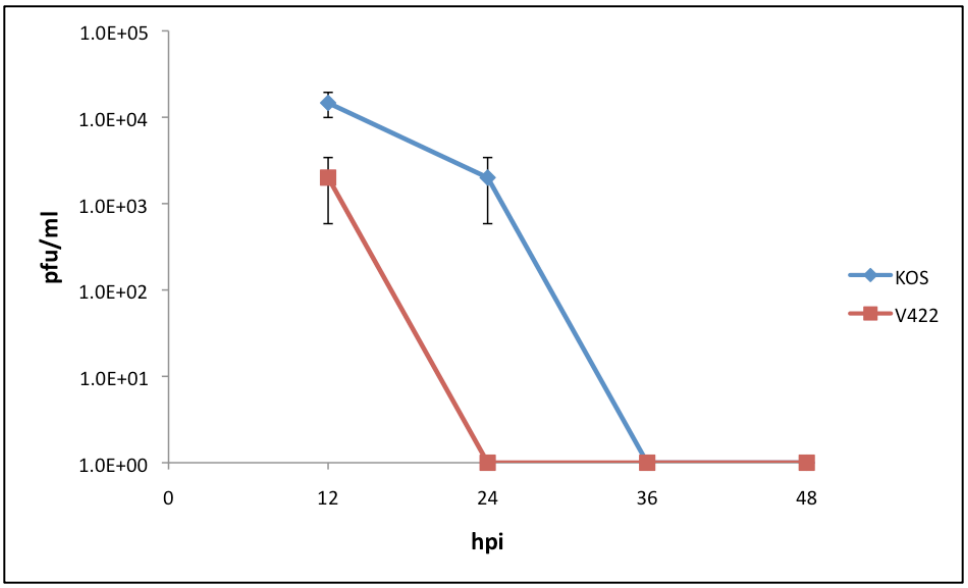

Figure 4.8 HSV replication in differentiated ONS-76 cells (+ACV)
ONS-76 cells were differentiated in 6-well plates and incubated with 100μM ACV beginning 24 hours prior to infection. Infection by HSV strain KOS or V422 was performed at an MOI of 1, and at the indicated time point cells were removed from the wells by scraping and processed for use in a plaque assay. ACV pressure was maintained throughout the experiment. Data points are an average of 2 replicates.

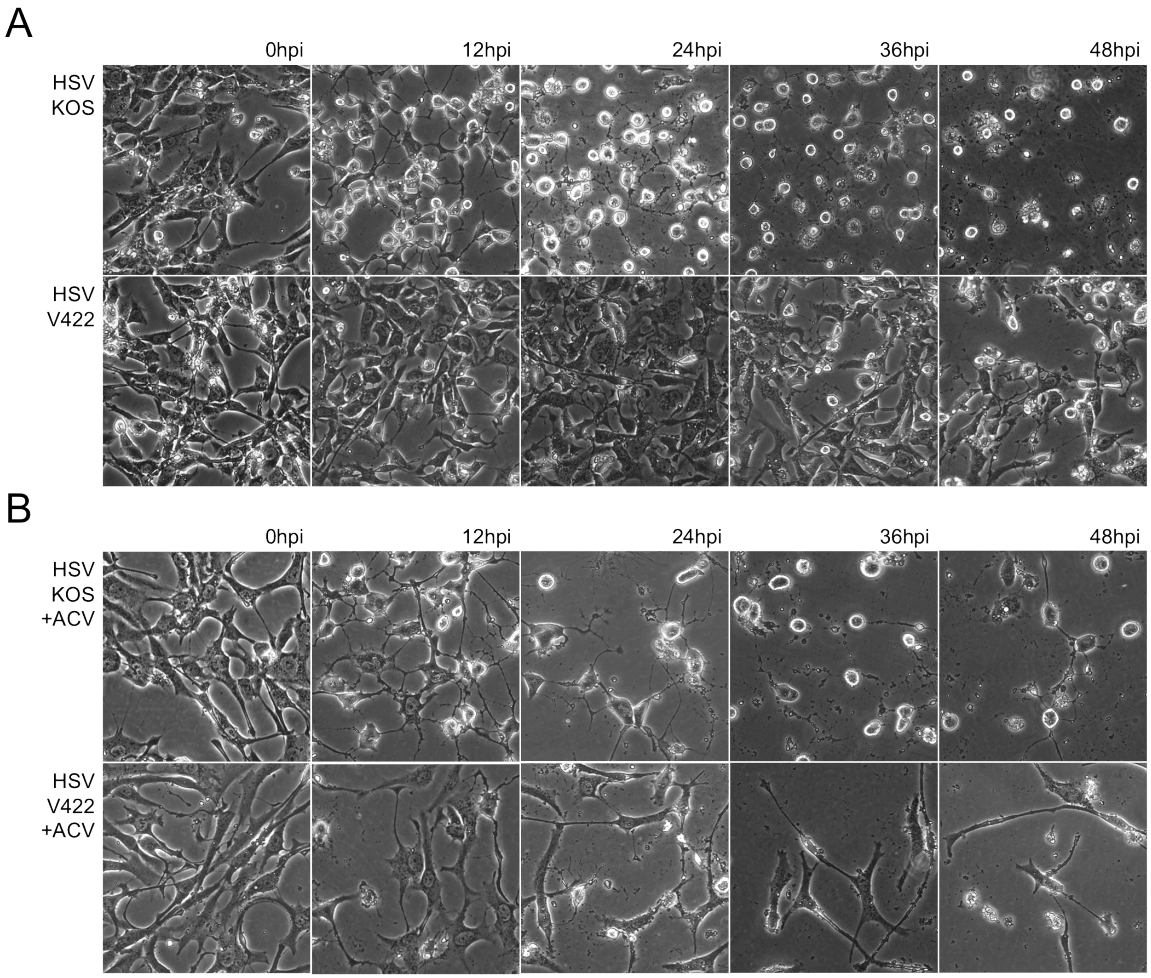

Figure 4.9 Morphology of differentiated ONS-76 cells during infection
ONS-76 cells were differentiated in 6-well plates and infected with the indicated HSV strain at an MOI of 1. At the indicated time point, cell cultures were visualized by confocal microscopy. Pictures depict a representative sample of cells in culture. A: KOS and V422 infection of differentiated ONS-76 cells B: KOS and V422 infection of differentiated ONS-76 cells in the presence of 100μM ACV.

4.2.2 Establishing quiescent HSV infection of differentiated UW228 cells

It was also determined if differentiated UW228 cells could support quiescent infection with wild type or mutant HSV. To resolve this, UW228 cells were differentiated and infected with HSV KOS or V422 at an MOI of 1. Infection was performed in the presence of ACV, and both viral titer and culture morphology were monitored over a seven day period. Titers of both KOS and V422 declined to undetectable levels as time progressed (Figure 4.10), with this process occurring more slowly than what was seen in infection of ONS-76 cells (Figure 4.8). Infectious V422 became undetectable by day 4 post infection, while KOS was found in cultures until day 7 (Figure 4.10). In KOS-infected cultures, CPE was observed to slowly spread throughout, with the vast majority of cells being lost by day 7 (Figure 4.11, top). In V422-infected cultures there was relatively minor development of CPE, and while cell density did initially decrease, viable cells were still abundant on day 7 (Figure 4.11, bottom). Based on this data differentiated cultures of UW228 cells appeared to tolerate infection with V422 and the virus was further investigated in this system.

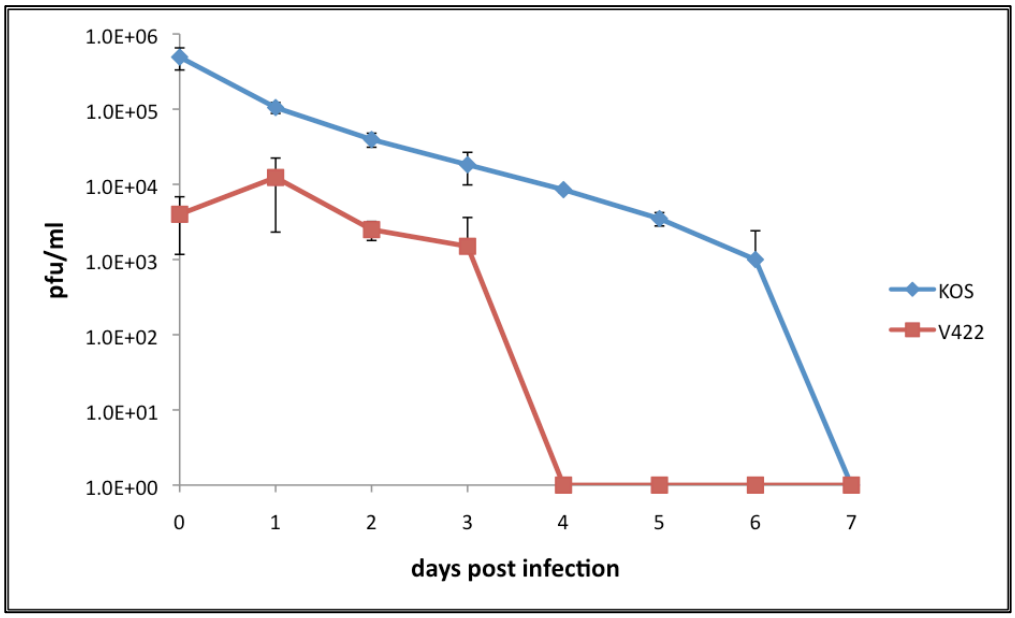

Figure 4.10 HSV replication in differentiated UW228 cells
UW228 cells were differentiated in 6-well plates and incubated with 100μM ACV beginning 24 hours prior to infection. HSV KOS and V422 were used to infect UW228 cells at an MOI of 1, and cells were harvested by scraping at the indicated time points. ACV pressure was maintained throughout the experiment, with culture media being refreshed on days 3 and 6. Detection of infectious virus was by plaque assay. Day 0 sample was harvested following the 1h incubation of input virus. Data points represent an average of 2 replicates.

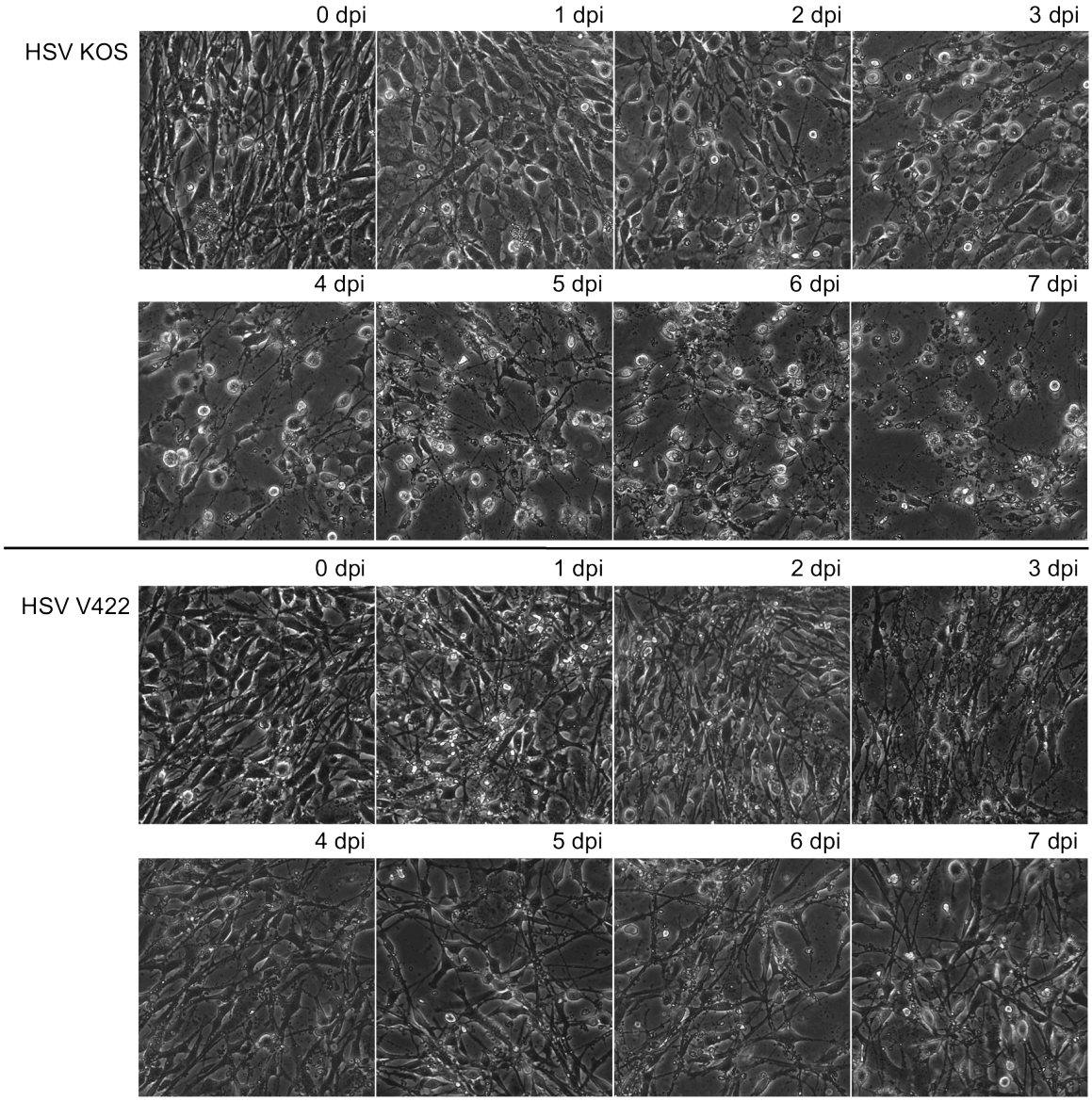

Figure 4.11 Morphology of HSV-infected differentiated UW228 cells
Differentiated UW228 cells were infected with HSV KOS or V422 at an MOI of 1 in the presence of 100μM ACV. ACV pressure was maintained throughout, and media was refreshed on days 3 and 6. At the indicated time point cultures were visualized by confocal microscopy. Images depict a representative sample of infected cells. Top: Infection of differentiated UW228 cells with KOS. Bottom: Infection of differentiated UW228 cells with V422.

As HSV V422 infection appeared to have limited toxicity on differentiated UW228 cells, viral transcription was assessed to characterize if this infection was consistent with quiescence. Transcription from the IE class gene ICP0, E class gene thymidine kinase (TK), and L class genes VP5 and VP16 was quantified by qRT-PCR to determine if lytic gene expression occurred. Expression from the LAT locus was also quantified, as the presence of this transcript correlates strongly with latency. All investigated lytic genes demonstrated increases ordered according to temporal class within the first 10 hours, with detection gradually decreasing to low or undetectable levels over the following 4 days (Figure 4.12). Transcription after day 4 was not observed for ICP0, VP5, and VP16, while low levels of TK transcripts continued to be detected even at 7 dpi (Figure 4.12). The LAT was not detected throughout the course of this experiment (Figure 4.12), however this result must be interpreted with caution as a positive control was not performed. As LAT expression is not strictly required to model latency, the pattern of lytic gene transcription observed in HSV V422 infection of differentiated UW228 cells was concluded to be consistent with quiescent infection.

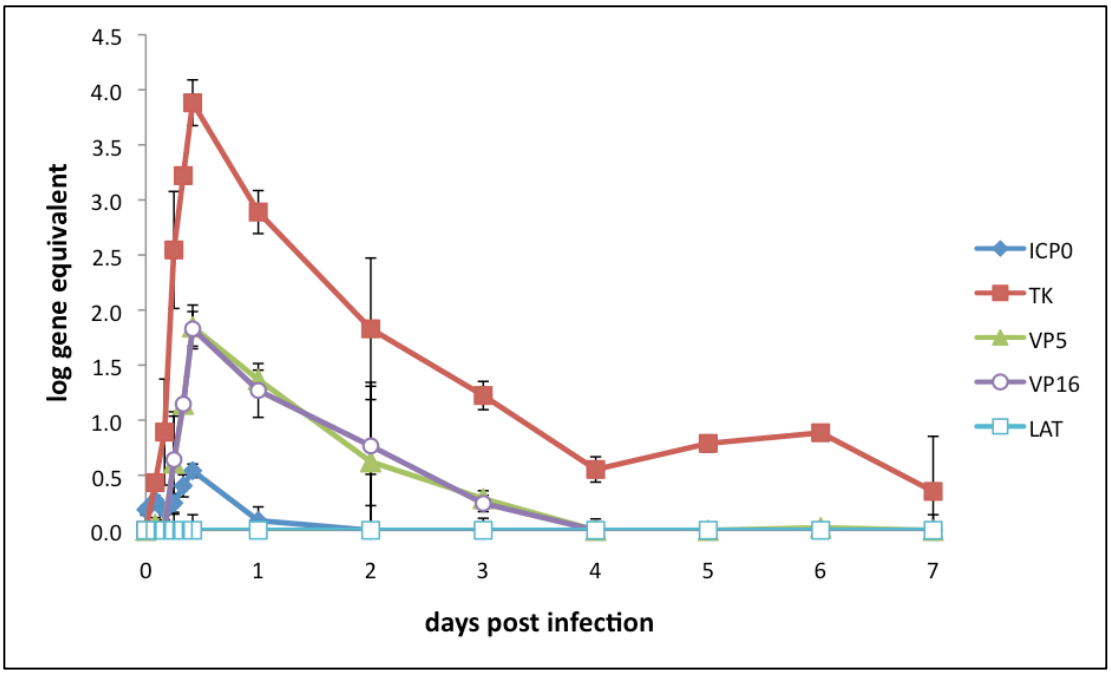

Figure 4.12 Transcription from HSV V422 in differentiated UW228 cells
Differentiated UW228 cells were infected with HSV V422 at an MOI of 1 in the presence of ACV and transcription from the virus was monitored for a 7 day period. At the indicated time points, supernatant was removed from wells and cells were harvested. RNA was isolated, quantified, converted to cDNA and quantified by qRT-PCR according to the protocol outlined in Methods. Gene equivalents for Ct values were generated through the use of standard curves specific to each primer set. Two wells were harvested for each time point and qRT-PCR was performed in duplicate, points represent the average of these data.

The results insofar depict HSV V422 infection of differentiated UW228 cells to be consistent with quiescence, as this system features the disappearance of lytic transcription and viral replication after an initial period of detection. To confirm that the HSV genome endured in the absence of infectious virus and lytic expression, the persistence of HSV DNA in long-term infection was investigated. Cultures of differentiated UW228 cells were infected with HSV V422, and the amount of viral DNA was quantified in total DNA over a 12 day period. Detection of V422 was observed to gradually decline as infection progressed, with the number of genomes being reduced by half between day 3 and day 12 (Figure 4.13). The number of genomes detected following inoculation was $2.2x10^6$ per million cells, therefore by day 3 only 1.47% of the input virus was detectable. This result confirms that viral DNA persists beyond the disappearance of infectious virus and lytic transcription, consistent with quiescence, however only a small fraction of input virus is detectable

throughout long-term infection. As the frequency of persisting genomes was low, the conformation of the remaining virus was investigated to determine if it was consistent with other defining characteristics of latency.

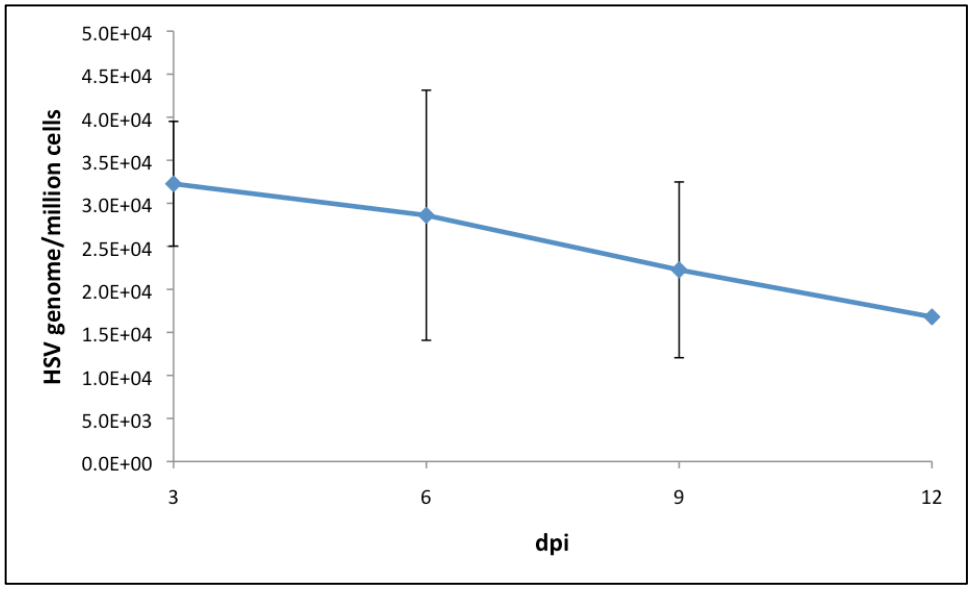

Figure 4.13 Persistence of HSV V422 in differentiated UW228 cells
Differentiated UW228 cells were infected with HSV V422 at an MOI of 1 in the presence of ACV. ACV pressure was maintained throughout, and media was refreshed on days 3, 6, and 9. At the indicated time point, cells were harvested by scraping and processed to isolate total DNA. Viral and cellular targets (VP16 and ZF) were quantified by qRT-PCR as detailed in Methods. Gene equivalent was determined through the use of standard curves generated for each specific primer set. The presence of viral target was not detected in mock infected cultures. Input virus detectable after inoculation procedure was $2.2x10^6$ viral genomes per million cells. Two wells were harvested for each time point and qRT-PCR was performed in duplicate for cellular and viral targets, points represent the average of these data.

The HSV genome is thought to exist as a circular episome during latent infection [28], and Gardella gels have long been used as a means of distinguishing the circular form of latent herpesviruses from other conformations [119]. Therefore, a Gardella gel was run in an attempt to distinguish whether the HSV genomes present in long-term infection of differentiated UW228 cells existed in a conformation characteristic of latent infection.

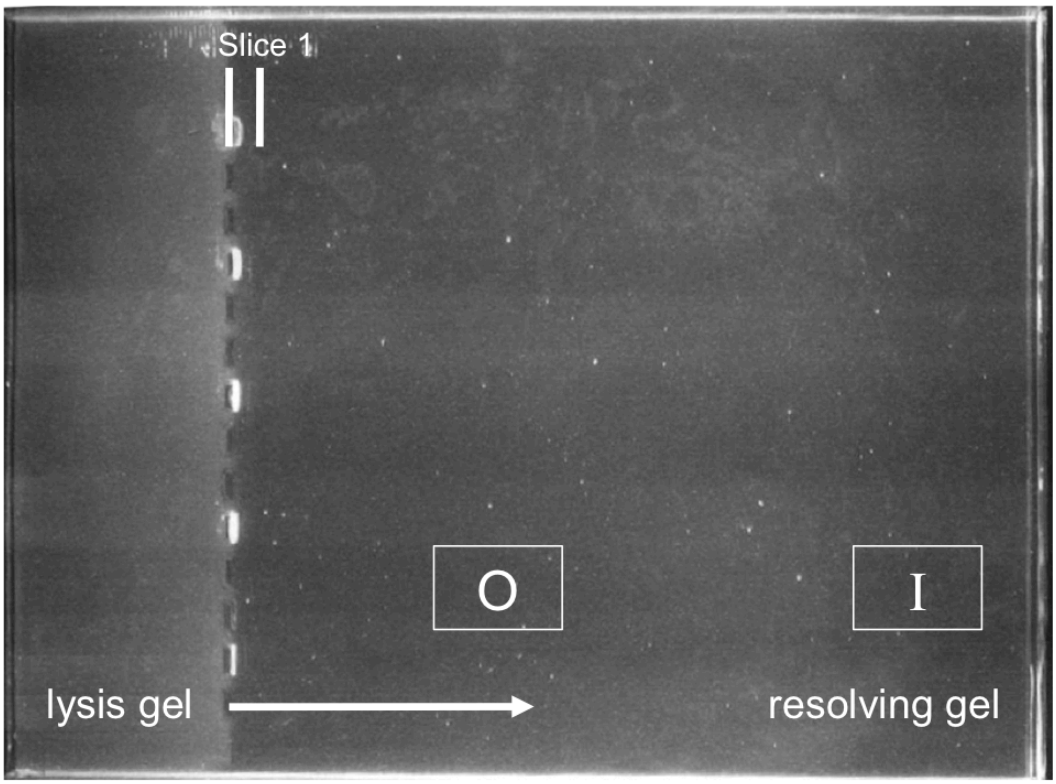

Figure 4.14 Gardella gel
Image of Gardella gel post-electrophoresis with UV illumination. Gardella gel was prepared and electrophoresed according to the procedure detailed in Methods. Bands represent cellular genomic DNA from loaded wells, O represents the approximate expected location of circularized HSV detection, and I represents the approximate expected location of linear HSV detection [105]. Each loaded lane was cut into 0.5cm sequential slices, with slice 1 containing the bottom of the Gardella gel wells, then used as template in PCR reactions.

Cultures of differentiated UW228 cells representing day 0, 7, 14, and 21 post HSV V422 infection were prepared and run in a Gardella gel as shown in Figure 4.14. Cultures of Vero cells infected for 6 hours with the HSV mutant n212 were included in this experiment, as this mutant has been demonstrated to adopt a circular format under such conditions [28]. PCR for detection of HSV DNA was performed on slices generated from individual

lanes of the Gardella gel, and reaction products visualized on agarose gels. HSV DNA was detected in slices 27-29, corresponding to approximately 14cm from the Gardella gel wells (Figure 4.15, Figure 4.16), which is consistent with migration of the linear form [105]. Viral DNA was detected in this region for day 0 and 7 cultures as well as n212 infection (Figure 4.15, Figure 4.16), but was not detected in day 14 and 21 cultures (Figure 4.16). The circular form of HSV migrates more slowly than the linear form and was expected to be detected approximately 5-6cm from the wells [105]. None of the PCR reactions performed on this region returned products, however, including those from this region of the HSV n212 positive control. Several of the lanes returned non-specific bands migrating at slightly less than 100bp, however only the bands migrating at 275bp represent the specific PCR product. As the amount of virus present in the tested cultures proved to be below the threshold of detection by the Gardella gel, no conclusion could be reached on the conformation of HSV V422 in long-term infection of differentiated UW228 cells.

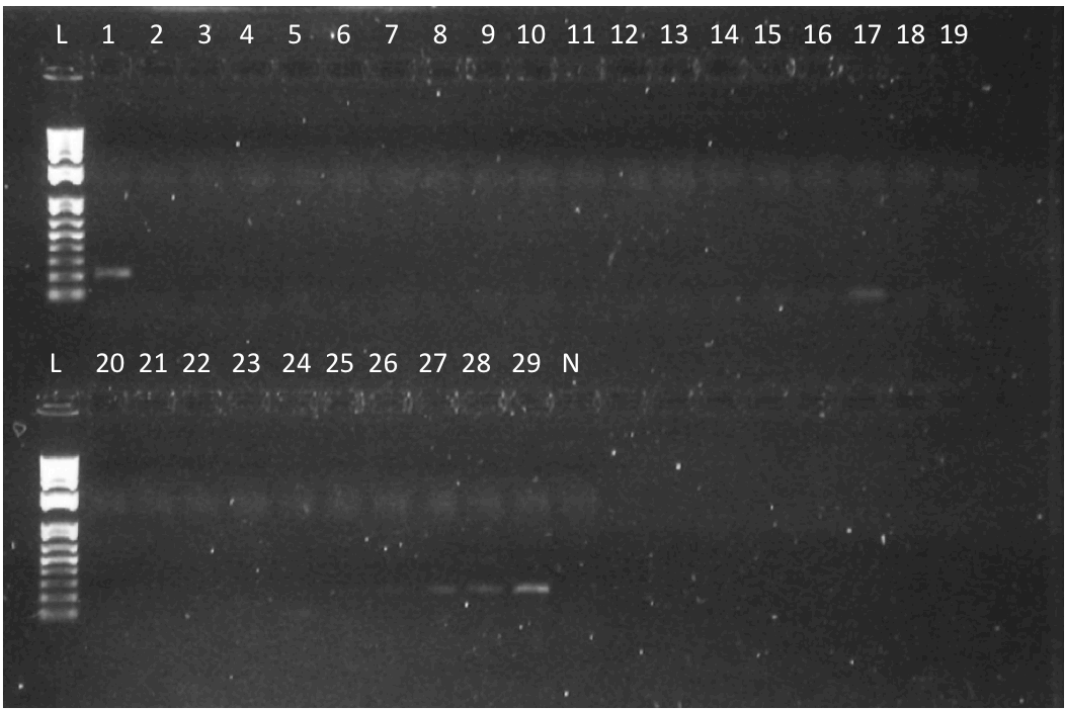

Figure 4.15 Detection of n212 in Vero cells by Gardella gel
Vero cells were seeded into 6-well plates at a density of $2x10^5$ cells/well and allowed to reach confluence. 24 hours prior to infection, media containing 100μM ACV was added. The HSV mutant n212 was used to infect the Vero cells at an MOI of 3 and infection was allowed to progress for 6 hours before cultures were prepared and loaded into the Gardella gel. Slices from the Gardella gel lane containing n212-infected Vero cells were used as template in PCR reactions as detailed in Methods, and products from these reactions were electrophoresed on the pictured agarose gel. Lanes marked L contain 100bp ladder. Lane numbers indicate the Gardella gel slice used as template and contain PCR reaction products. Lane N contains products from the control (no template) PCR reaction. Slice 17 reaction products contain a non-specific band of <100bp.

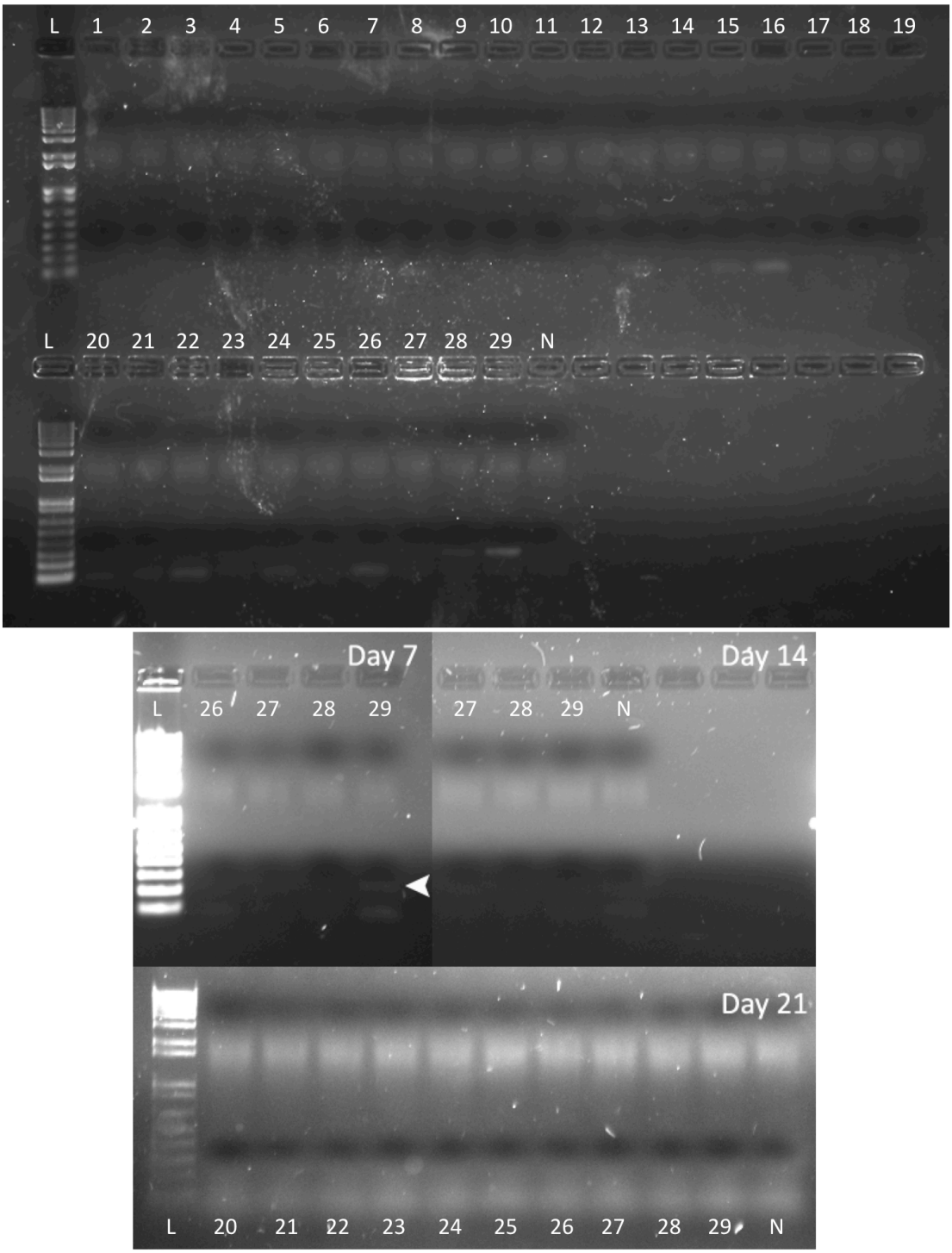

Figure 4.16 Detection of V422 in UW228 cells by Gardella gel
UW228 cells were differentiated and infected with HSV V422 at an MOI of 1 in the presence of ACV. Infection was allowed to progress for the indicated time intervals with maintained ACV pressure before cells were prepared and loaded into the Gardella gel. Slices from the appropriate Gardella gel lanes were used as template in PCR reactions as detailed in Methods, and products from these reactions were electrophoresed on the pictured agarose gels. Day 0: Lanes marked L contain 100bp ladder. Lane numbers indicate the Gardella gel

slice used as template and contain PCR reaction products. Lane N contains products from the control (no template) PCR reaction. Specific band is indicated by white arrowhead. Day 7: Lane L contains 100bp ladder, numbered lanes contain products from slices 26-29. Specific band is indicated by white arrowhead. Day 14: Products from slices 27-29, lane N contains products from no template PCR reaction. Day 21: Products from slices 20-29. Lane L contains 100bp ladder, lane N contains products from no template PCR reaction.

4.3 Reactivation of HSV in differentiated medulloblastoma cells

The third aim of this project was to determine if HSV reactivation could be modeled in differentiated medulloblastoma cells. Drawing on recent reports indicating distinct profiles of HSV transcription in productive infection and reactivation [62, 63], it was evaluated if differentiated ONS-76 cells could simulate the environment of a neuron post-reactivation stress. Long-term HSV infection of differentiated UW228 cells was also evaluated for reactivation using a similar approach to what has been described in the PC-12 cell model [84].

4.3.1 Reactivation-type transcription in differentiated ONS-76 cells

ONS-76 cells demonstrated differentiation along a neuronal pathway (Section 4.1), however proved unsuitable for hosting long-term HSV infection (Section 4.2.1). As tumour cells must inherently deal with genotoxic and metabolic stresses, one explanation for the incompatibility of HSV quiescence with differentiated ONS-76 cells is that these cells are locked in a state of stress. To explore this hypothesis it was determined if HSV infection of differentiated ONS-76 cells resembled reactivation. It has been shown that HSV undergoing reactivation deviates from the temporal transcription cascade of productive infection, with simultaneous expression from all lytic gene classes [62]. To determine the HSV gene expression profile in this system, differentiated ONS-76 cells were infected with HSV KOS or V422 at an MOI of 1 and lytic gene expression was assessed by qRT-PCR. As HSV undergoes productive replication in MRC-5 cells, infection in this cell line served as a control example of lytic expression.

During lytic HSV infection transcription proceeds from IE to E to L gene classes, and this order was observed during infection of MRC-5 cells with wild type virus (Figure 4.17, top). ICP0, from the IE class, reached its maximum at 2hpi followed by TK (E) at 4hpi and VP5/VP16 (L) at 6hpi. This pattern of transcription was also observed in KOS infection of differentiated ONS-76 cells (Figure 4.17, bottom), with lytic transcripts reaching maximum values in the same temporal order as in MRC-5 cells. In HSV V422 the activation domain of VP16 is deleted, preventing the virus from counteracting intrinsic cellular repression of IE gene transcription, and blocking entry into the lytic expression cascade. HSV V422 infection of MRC-5 cells exhibited low levels of transcription from all lytic gene classes, which

decreased from initial detection levels as time progressed (Figure 4.18, top). This result is expected to be observed if, in the absence of VP16 induction, the virus is unable to overcome the barrier to transcription enacted by cellular repression mechanisms. In contrast, infection of differentiated ONS-76 cells with V422 resulted in a simultaneous increase in transcription from all classes occurring at 4hpi (Figure 4.18, bottom). This gene expression profile is consistent with what has been observed during HSV reactivation in other systems [62, 63], and is the first indication that reactivation-type replication may be modeled in cell culture without requirement for latency establishment and maintenance.

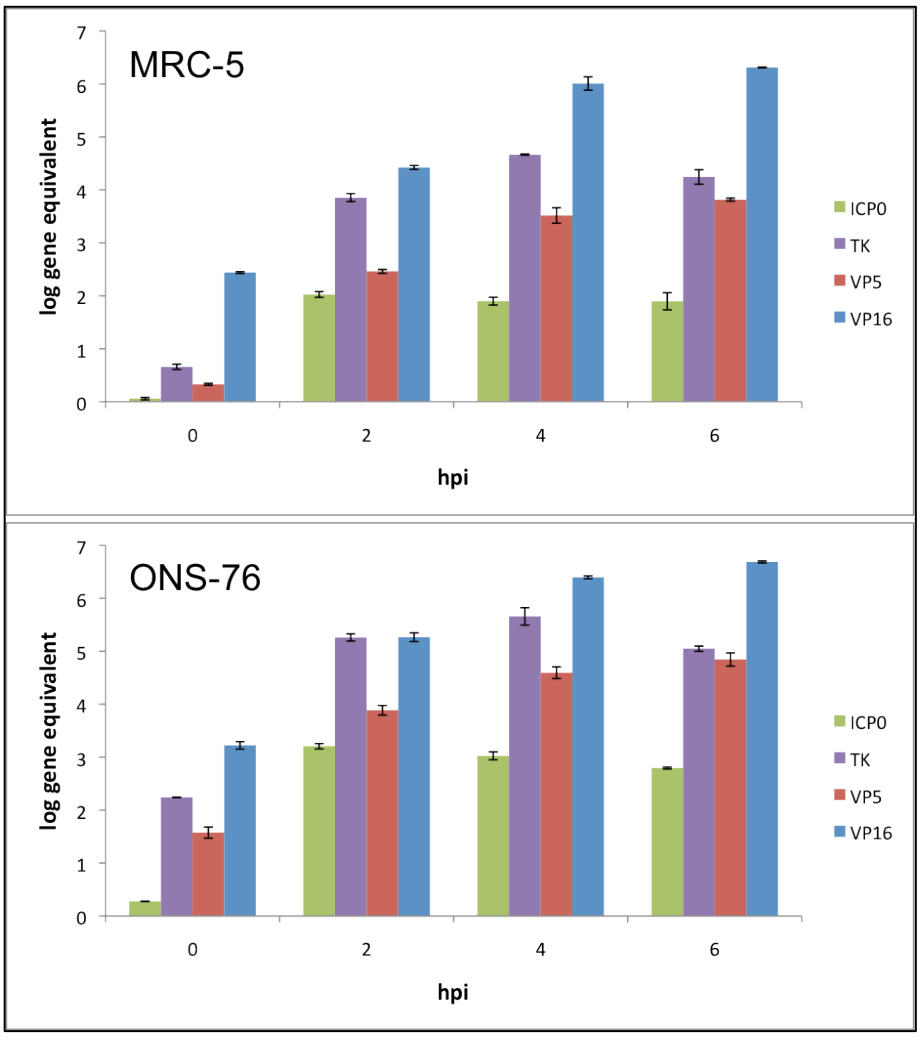

Figure 4.17 Gene expression of HSV KOS in differentiated ONS-76 and MRC-5 cells
ONS-76 cells were differentiated in and MRC-5 cells were allowed to reach confluence in 6-well plates. Cultures were infected with HSV KOS at an MOI of 1 and transcription from the virus was monitored over the following 6 hour period. At the indicated time points the

supernatant was removed and cells were harvested. RNA was isolated, quantified, and converted to cDNA as described in Methods. qRT-PCR was performed on a standardized amount of cDNA for each of the genes depicted, and Ct values were converted to gene equivalent through use of primer-specific standard curves. Data represents an average of duplicate PCR reactions from two wells per time point. Top: transcription from KOS in MRC-5 cells. Bottom: transcription from KOS in differentiated ONS-76 cells.

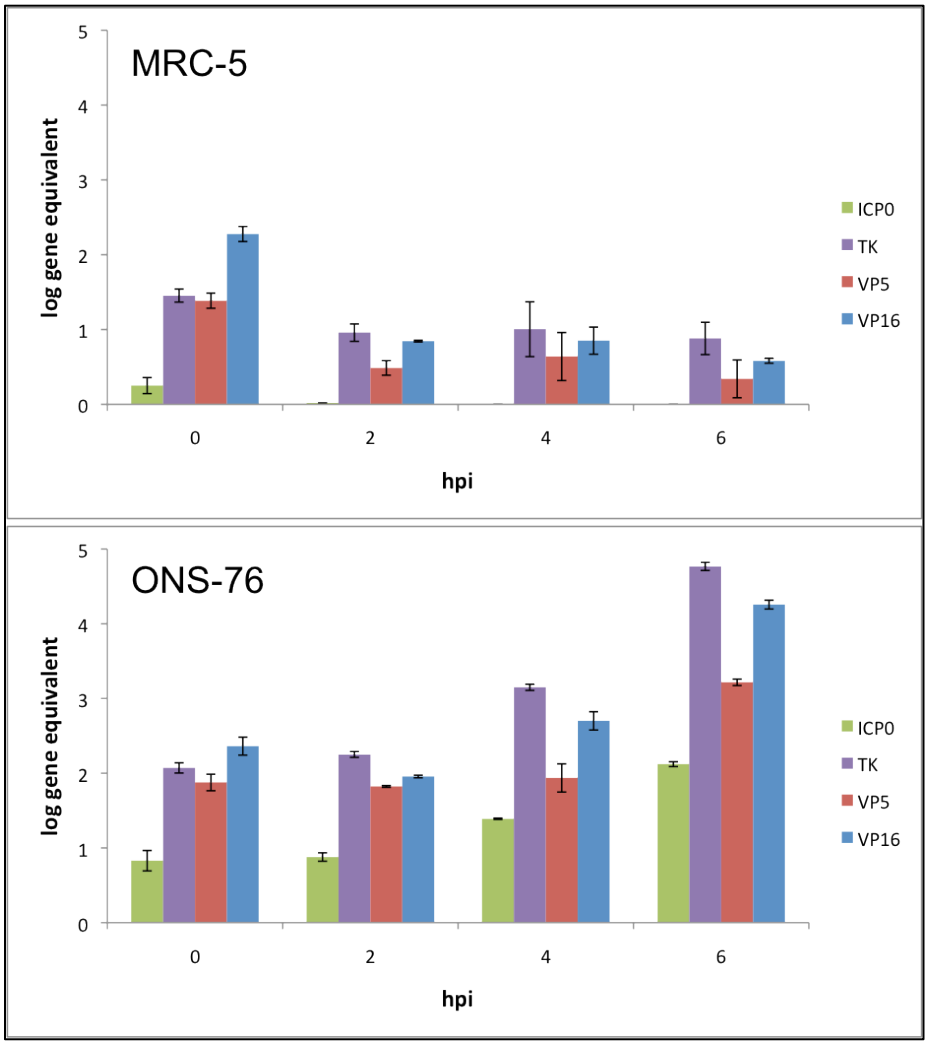

Figure 4.18 Gene expression of HSV V422 in differentiated ONS-76 and MRC-5 cells
ONS-76 cells were differentiated in and MRC-5 cells were allowed to reach confluency in 6-well plates. Cultures were infected with HSV V422 at an MOI of 1 and transcription from the virus was monitored over the following 6 hour period. At the indicated time points the supernatant was removed and cells were harvested. RNA was isolated, quantified, and converted to cDNA as described in Methods. qRT-PCR was performed on a standardized amount of cDNA for each of the genes depicted, and Ct values were converted to gene equivalent through use of primer-specific standard curves. Data represents an average of duplicate PCR reactions from two wells per time point. Top: transcription from V422 in MRC-5 cells. Bottom: transcription from V422 in differentiated ONS-76 cells.

4.3.2 Reactivation from quiescence in differentiated UW228 cells

Viral genomes were shown to persist in V422 infection of differentiated UW228 cells (Section 4.2.2), and this virus was assessed for the ability to respond to reactivation stimuli by re-entering the replicative cycle. Figure 4.19 outlines the procedure used for the reactivation experiments detailed herein. Briefly, long-term V422 infection of differentiated UW228 cells was established and the virus subjected to a variety of reactivation stimuli. Total DNA was purified from cultures for 7 days following reactivation stress, and cellular and viral targets in the harvested DNA were quantified by qRT-PCR. In this manner, viral DNA amplification in response to reactivation stress could be used as a sensitive assessment of reactivation.

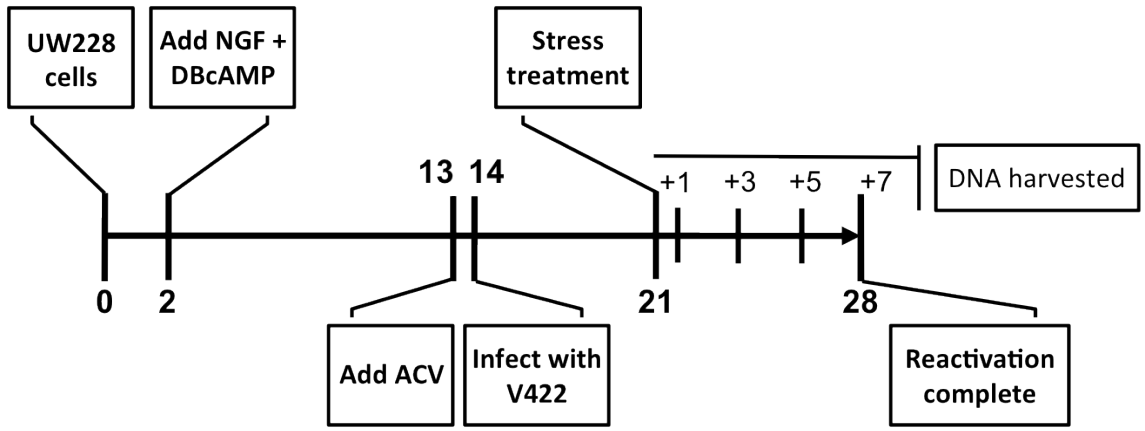

Figure 4.19 Outline of reactivation experiments

Reactivation stress was achieved by exposure to forskolin or trichostatin A (TSA), superinfection with UV-inactivated HSV, transfection with an adenovirus expression vector carrying Luman (Ad.Luman) or LacZ (Ad.LacZ), and heat shock. Forskolin, TSA, and heat shock are common methods of inducing HSV reactivation [74, 120, 121], while superinfection with UV-inactivated HSV was used to deliver wild-type VP16 protein to the quiescent virus. Luman is a cellular homologue of VP16 that can activate IE gene expression under certain conditions [122], and was included as a potential reactivation stimulus. Antiviral pressure was removed at the time of exposure to reactivation stimuli to permit viral DNA replication, and V422-permissive U2OS cells were seeded into the infected UW228 cultures post-stress to amplify successful reactivation events. As the differentiation

agents DBcAMP and NGF were selectively toxic to the overlaid U2OS cells, these chemicals were not maintained in culture media following reactivation stress.

Three outcomes were observed in cultures following reactivation stress: no change in cell density or morphology, some decrease in cell density accompanied by scattered cells displaying CPE, or death of the majority of cells in culture. Stress stimuli resulting in culture death included treatment with TSA and transfection with Ad.Luman (Figure 4.20A). Both treatments resulted in the vast majority of cells becoming round and detaching from the plate surface, a phenomenon consistent with cell death, within 3 days of reactivation stress. Treatments which appeared to have no effect on culture morphology included removal of differentiating agents alone, and application of forskolin (Figure 4.20B). Cultures in these treatment groups exhibited identical morphology on days 0 and 7 post reactivation, with similar or slightly increased cell densities. Finally, treatment with UV-inactivated HSV, Ad.LacZ, and heat shock resulted in some decrease in cell density with scattered cells displaying CPE (Figure 4.20C). Substantially more CPE was observed in cultures superinfected with UV-inactivated HSV over the other treatments. Prior to this study the radiation dose required to fully inactivate the virus was determined. In this experiment however, controls containing only UV-inactivated HSV demonstrated the same spreading CPE as test cultures. This result indicates that the UV-inactivated virus stock retained residual replicative ability, obscuring the effects of providing wild type VP16 to the V422 genome.

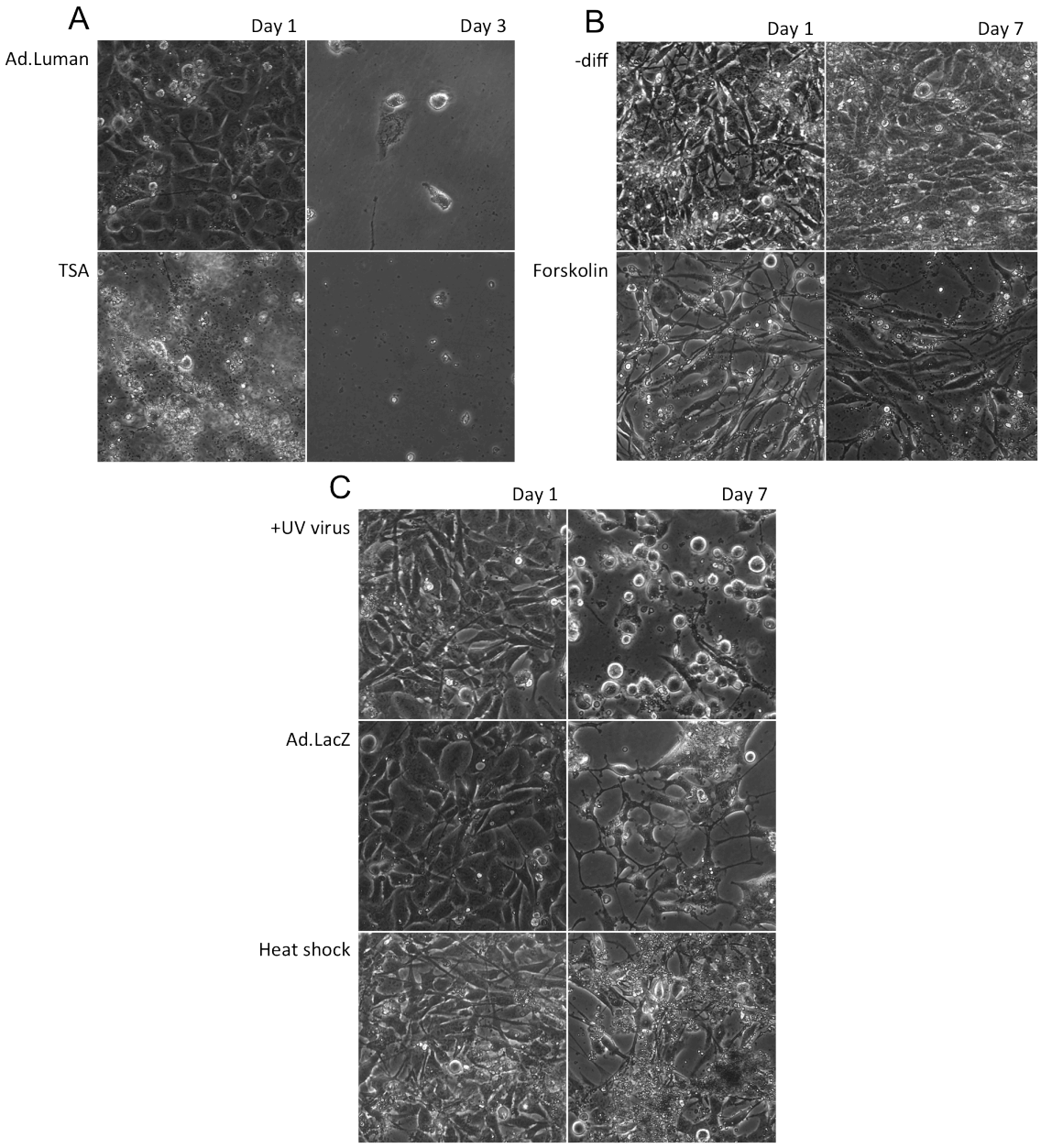

Figure 4.20 Morphology of V422-infected UW228 cells following reactivation stimuli
UW228 cells were differentiated and infected with HSV V422 as outlined in Figure 4.19. U2OS cells were overlaid at a density of $2x10^5$ cells/well following stress treatment. Images were captured daily for 7 days after reactivation stimulus (reactivation day 0) and depict a representative sample of the visualized cultures. A: reactivation treatments resulting in cell death. B: reactivation treatments with no discernable effect on culture morphology. C: reactivation treatments resulting in loss of cell density and CPE. Note: Forskolin-treated UW228 cells were not overlaid with U2OS cells.

The number of HSV genomes present in V422-infected UW228 cultures post-reactivation was examined to assess if stress treatment induced viral DNA amplification. The cell death observed following treatment with TSA and transfection with Ad.Luman was not accompanied by a substantial increase in viral genomes (Figure 4.20A, Figure 4.21, Table 4.3). Conversely, removal of differentiating agents from cultures did not appear to result in the development of CPE (Figure 4.20B) yet an increase in viral DNA was observed by day 7 (Figure 4.21, Table 4.3). A plaque assay was performed on lysates of forskolin-treated cells to determine if this reactivation stimulus resulted in the emergence of infectious virus. Infectious virus was not detected, and the more limited sensitivity of the plaque assay precludes comparison to treatments assessed by PCR. Heat shock induced the greatest amplification of viral DNA (Figure 4.21), consistent with the development of scattered CPE in culture morphologies (Figure 4.20C). Superinfection of differentiated UW228 cells with UV-inactivated HSV resulted in a substantial increase in viral DNA (Figure 4.22, Table 4.3), which is consistent with indications that the UV-inactivated virus stock retained a degree of replicative competence. Transfection with Ad.LacZ resulted in some elevation in HSV genomes detected at day 7 (Figure 4.21, Table 4.3), although this result does not explain the initial loss in cell density and development of CPE observed in culture morphologies (Figure 4.20C). In sum, these results demonstrate that amplification of HSV V422 DNA in differentiated UW228 cells occurred after treatment with heat shock, removal of differentiating agents, and, to a lesser extent, after transfection with a control adenovirus expression vector.

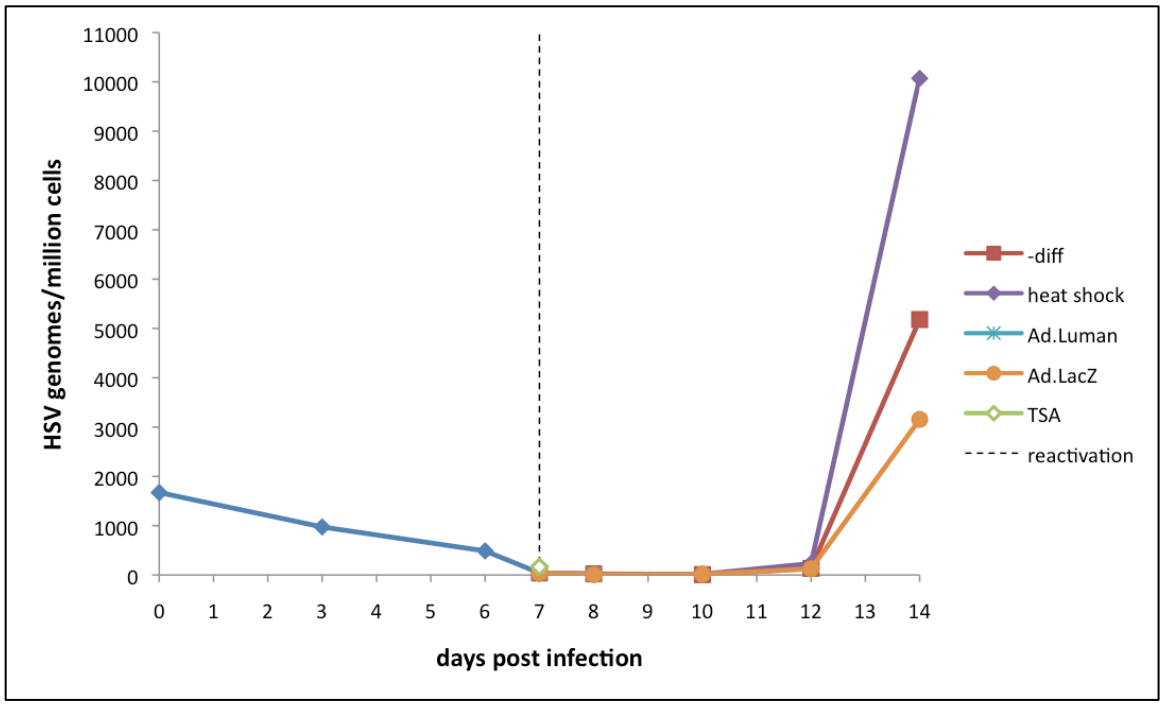

Figure 4.21 Amplification of HSV V422 in response to reactivation stimuli
UW228 cells were differentiated and infected (day 0) as outlined in Figure 4.19. The presence of HSV V422 in cultures was monitored through the establishment phase (days 0-7) and following reactivation stimuli (days 7-14) by extracting total DNA from cells and performing qRT-PCR as detailed in Methods. On day 7 differentiating agents and ACV were washed out and cells exposed to the indicated stress treatments, following which $2x10^5$ U2OS cells/well were added to cultures. Treatment conditions: -diff; ACV and differentiating agents removed from cultures with no additional stress treatment. Heat shock; cultures incubated at 43°C for 3h. Ad.Luman; adenovirus expression vector carrying exogenous Luman infected at an MOI of 100. Ad.LacZ; same conditions as Ad.Luman. TSA; 60ng/ml TSA added to media.

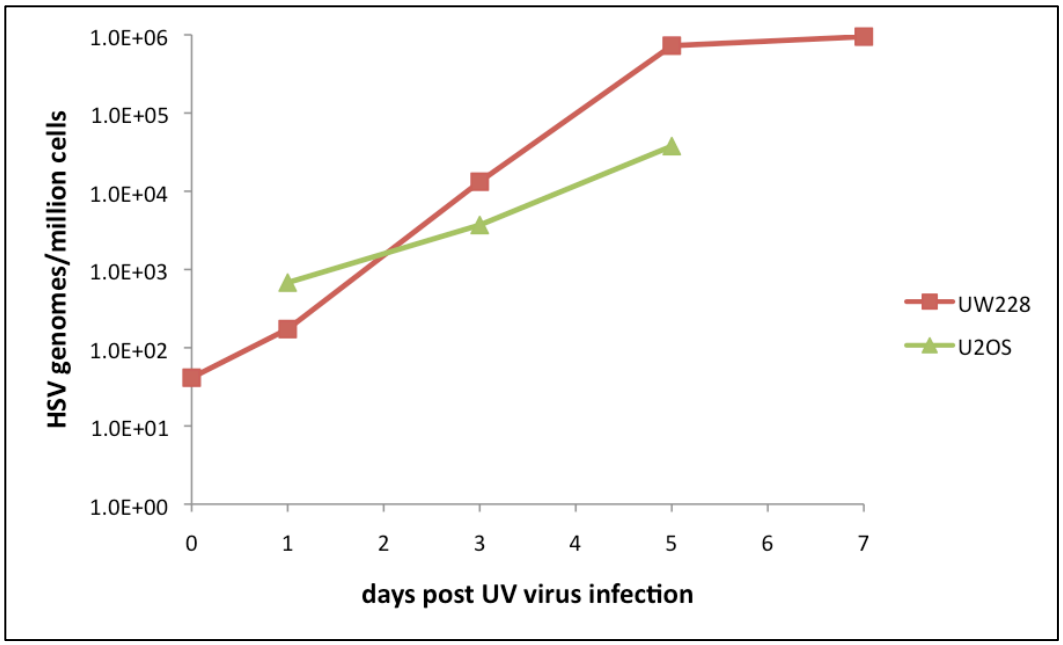

Figure 4.22 Viral amplification after superinfection with UV-irradiated HSV
UW228 cells were differentiated and infected as outlined in Figure 4.19. For reactivation stress, HSV KOS stock was subjected to $1x10^6 \mu J/cm^2$ UV radiation in a Stratagene UV Stratalinker 1800 and used to superinfect cultures of V422-infected UW228 cells or U2OS cells at an MOI of 1 (as calculated from the titer of non-irradiated stock). UW228 cells were then overlaid with $2x10^5$ U2OS cells/well. At the indicated time points cells were harvested by scraping and total DNA was extracted and processed for qRT-PCR as detailed in Methods. Genome equivalents were determined by standard curves specific to each primer set, and the number of viral DNA copies per million cells calculated.

Table 4.3 Quantification of HSV and UW228 cells after exposure to reactivation stimuli

Stimulus	Target	Initial (genome equivalent)	Final (genome equivalent)
Day 7 (pre-stress treatment)	Viral	29	-
	Cellular	$7.4x10^5$	-
-ACV/-diff	Viral	16	$1.4x10^4$
	Cellular	$6.7x10^5$	$3.5x10^6$
+UV virus	Viral	236	$5.6x10^4$
	Cellular	$1.3x10^6$	$6.3x10^4$
Heat shock	Viral	17	$2.7x10^4$
	Cellular	$9.4x10^5$	$2.0x10^6$
Ad.Luman	Viral	11	6
	Cellular	$6.6x10^5$	$4.1x10^3$
Ad.LacZ	Viral	11	$4.1x10^3$
	Cellular	$1.4x10^6$	$1.1x10^6$
TSA	Viral	23	85
	Cellular	$2.9x10^4$	$4.8x10^3$

Initial and final genome equivalents observed after reactivation treatments (experiment detailed in Figure 4.21). VP16 (viral target) and ZF (cellular target) copies were quantified in total DNA as an indication of the number of viral and cellular genomes present. Initial genome equivalents represent viral and cellular genome copies detected on day +1 post reactivation stress (excepting day 7, which is pre-stress treatment and day 0 of reactivation). Final genome equivalents represent viral and cellular genome copies detected on day +7 following reactivation or the last day cells were observed in culture (day +3 for Ad.Luman and TSA). Two wells were harvested for each treatment at each time point and qRT-PCR was performed in duplicate, numbers represent the average of this data.

Chapter 5 Discussion

One strategy in developing *in vitro* models of HSV latency and reactivation has been to induce neuronal differentiation from a proliferating precursor cell, as in the case of the PC-12 model. Medulloblastomas originate in the human CNS and can be induced to differentiate along a neuronal pathway [91, 95, 96], therefore cell lines derived from these tumours were examined for their use as a model of HSV latency and reactivation. ONS-76 and UW228 medulloblastoma lines were induced to differentiate and the parameters of establishing quiescent HSV infection in these cells were explored. Differentiated ONS-76 cells were found to be incompatible with hosting quiescent HSV infection, however peculiarities observed in the behaviour of HSV in this study may yield significant results. Differentiated UW228 cells were found to be capable of hosting quiescent HSV infection that could further be induced to re-enter productive replication, although certain restrictions were necessary to achieve this. The results collectively demonstrate that differentiated medulloblastoma cells represent another perspective through which HSV latency and reactivation may be explored.

5.1 Differentiation of medulloblastoma cell lines

The first aim of this project was to develop human medulloblastoma tumour cell lines into neuronally differentiated cells. Of the three cell lines screened for neuronal differentiation capacity, morphological differentiation could be induced in ONS-76 and UW228 cells (Figure 4.1, Table 4.2). Differentiation of these two lines was characterized by analyzing proliferation rate (Figure 4.2, Figure 4.3) and assessing the expression of cell type marker proteins (Figure 4.4, Figure 4.5). Cultures of differentiated ONS-76 cells exhibited reduced proliferation as compared to control cells (Figure 4.2) and were induced to express the neuronal protein β-tubulin upon differentiation (Figure 4.4B). From this it was concluded that treatment with a combination of DBcAMP and resveratrol resulted in neuronal differentiation of ONS-76 cells. Cultures of differentiated UW228 cells also exhibited reduced proliferation as compared to control cells (Figure 4.3), however did not demonstrate increased expression of any tested marker protein (Figure 4.4D, E, Figure 4.5). Based on the observation that UW228 cells maintained expression of the neuron-

specific proteins Brn3A and NeuN throughout differentiation (Figure 4.5), it was concluded that these cells did possess neuronal character although treatment with DBcAMP and NGF did not cause further progression along a neuronal differentiation pathway.

A complicating result observed for both ONS-76 and UW228 cells was the ready detection of GFAP, a protein characteristic of glial cells (Figure 4.4). The original reports describing establishment of these cell lines note an absence of GFAP expression [110, 111], raising the possibility that ONS-76 and UW228 cells used in this study may have since migrated along a glial differentiation pathway. Glial differentiation is known to suppress responsiveness to neuronal differentiation stimuli [95], and offers an explanation for the observed absence of neurofilament (Figure 4.4, Figure 4.5). Alternatively, given that astrocyte precursor cells undergo stellation when treated with DBcAMP [123, 124], and considering the readily apparent GFAP expression, it is possible that the differentiated cells of this study more accurately represent astrocytes than neurons. As astrocytes are known to be permissive to HSV infection [125, 126], medulloblastoma cells that have moved towards glial differentiation may be less suitable for examining HSV latency and reactivation. Given the ambiguity in character displayed by differentiated ONS-76 and UW228 cells, a clear categorization cannot be made using the available data. As proteins associated with neuronal cells were detected, indicating some degree of neuronal bias, and because of the stability of the differentiated cells, differentiated ONS-76 and UW228 cells were nevertheless assessed for their compatibility with hosting HSV latency.

5.2 HSV reactivation and latency in differentiated ONS-76 cells

The medulloblastoma cell line ONS-76 was determined to differentiate, including expression of the neuron-associated protein β-tubulin, by treatment with a combination of DBcAMP and resveratrol. The differentiated ONS-76 cells were assessed for the ability to host quiescent HSV infection. While treated ONS-76 cells were found incompatible with use as a model of HSV latency, the results suggest these cells may be useful in studying reactivation-type replication of the virus.

5.2.1 Establishing quiescent HSV infection

The requirements for establishing quiescent HSV infection in differentiated ONS-76 cells were examined using wild type (KOS) and mutant (V422) viruses. When differentiated cells were infected, HSV KOS replicated as in a permissive system and HSV V422 replicated similarly to the wild type virus (Figure 4.7). HSV V422 is known to replicate poorly in non-complementing cells owing to the loss of the VP16 activation domain function [87], and its demonstrated ability to replicate in this system suggests that the mechanisms by which these cells repress the incoming virus may be defective—as is the case in U2OS cells [127]. The permissive state of U2OS cells to V422 replication has been linked to a deficit in inhibitory factors that repress the incoming virus in untransformed cells, factors which are presumably targeted by VP16 under normal circumstances [128]. Curiously, previous work in this laboratory has indicated that wild type HSV replication in undifferentiated ONS-76 cells is restricted [129], suggesting changes induced by differentiation may facilitate viral replication. The use of viral replication inhibition during infection caused titers of both HSV KOS and V422 to fall to undetectable levels within the first 36 hours of infection (Figure 4.8). This observation is consistent with entry into quiescence, however infected cultures developed widespread CPE and cell death was complete by 48hpi (Figure 4.9B). Cellular toxicity in the absence of viral replication is known to be mediated by the presence of IE gene products, which are synthesized even in the absence of HSV DNA replication [130, 131]. From these observations it was concluded that cell death was triggered by HSV infection of differentiated ONS-76 cells in the absence of viral replication, and this system was therefore incompatible with use as a model of HSV latency.

5.2.2 Reactivation-type replication

Because of the stress inherent to unregulated growth and carriage of multiple genetic aberrations, tumour cells may be better suited to modeling the neuronal environment after the experience of reactivation stress. It has been demonstrated that HSV responds to reactivation stress with a transcription profile distinct from that of lytic replication [62, 63], therefore the pattern of HSV transcription in differentiated ONS-76 cells was determined. HSV KOS displayed a pattern of gene expression nearly identical to the transcription profile observed in lytic infection of the fibroblast cell line MRC-5 (Figure

4.17). Following infection with HSV V422 low levels of viral transcription were detected in MRC-5 cells (Figure 4.18), consistent with the poor growth of VP16 AD mutants observed in most cell lines [132]. During infection of differentiated ONS-76 cells by HSV V422 however, transcripts accumulated from all kinetic gene classes simultaneously (Figure 4.18). This finding appears to contrast with the accumulation of HSV V422 transcripts in the permissive U2OS cell line, where ordered lytic gene expression is observed [127], suggesting that reactivation-type viral expression may be occurring in differentiated ONS-76 cells. This would represent a novel system for the study of stress and HSV reactivation induction; however reaching a firm conclusion entails resolving the requirement of early and late gene transcription for the immediate-early proteins in these results.

In the expression profiling experiments detailed herein, a relatively large number of viral transcripts were detected at time 0 for both viruses in ONS-76 and MRC-5 cells (Figure 4.17, Figure 4.18). As time 0 samples were collected upon inoculation and preceded viral entry, it is possible that the values obtained represent contaminating DNA from the relatively large number of input genomes present at this time point. This considered, the conclusions stand that in differentiated ONS-76 cells wild type HSV replicates as per the lytic transcriptional program and HSV V422 via a deviant pattern of gene expression. Further, the results indicate the gene expression profile of HSV V422 to be similar to what is observed during HSV reactivation.

5.3 HSV reactivation and latency in differentiated UW228 cells

The UW228 medulloblastoma cell line was determined to differentiate into cells that retained neuronal character when treated with a combination of NGF and DBcAMP, and the use of these differentiated cells as a model of HSV latency was assessed. Cultures of differentiated UW228 cells were found to stably host infection with mutant HSV, and the virus was examined for its ability to establish and reactivate from latency in this system using a traditional approach.

5.3.1 Establishing quiescent HSV infection

The requirements for establishing quiescent infection in differentiated UW228 cells were determined for both HSV KOS and HSV V422. Infection of differentiated UW228 cells in the presence of viral replication inhibition resulted in HSV KOS titers gradually declining

from input levels over the course of 7 days (Figure 4.10). Cultures infected with KOS also exhibited spreading CPE until cell death was complete (Figure 4.11). One explanation of these results is that small amounts of viral replication escaped restriction by ACV, however this is not supported by the transcription profile of the wild type virus. As cell death occurred in the absence of lytic transcription it was concluded that HSV KOS infection of differentiated UW228 cells was not compatible with establishing quiescence.

Differentiated UW228 cells were also infected with HSV V422 in the presence of replication inhibition, and viral titers were observed to decline to undetectable levels by day 4 (Figure 4.10). Some cell loss was observed during the initial days of infection (Figure 4.11), however the mutant virus had an overall mild effect on culture health. As these results were consistent with the virus entering quiescence, the transcriptional profile of HSV V422 under these infection conditions was characterized. An initial peak of lytic gene expression was observed, followed by a drop to low or undetectable levels in concert with the disappearance of infectious virus from culture (Figure 4.12). Transcription from the TK gene (induced by IE gene ICP4) remained detectable even at day 7 (Figure 4.12), suggesting that the virus persisted in culture. Similar low levels of TK transcription are detectable in latently infected neurons [133] although the etiology of these transcripts has not yet been resolved. The LAT was not detected above background levels at any time point analyzed (Figure 4.12), although this must be interpreted with caution in the absence of a positive control. While expression of the LAT is associated with quiescence [134], it is known that LAT-positive neurons do not represent the full number of neurons harboring latent HSV [135], and that HSV latency can be established in the absence of a functional LAT locus [37]. Collectively these results depict HSV V422 infection of differentiated UW228 cells to feature an initial period of lytic expression and detection of infectious virus, followed by a second phase where infectious virus is not present yet low levels of TK expression can be measured. This situation is consistent with quiescent HSV infection.

In order to quantify and characterize HSV V422 in long-term infection of differentiated UW228 cells, the amount and conformation of persisting viral DNA was determined. Persistence of the V422 genome in infected cultures was examined (Figure 4.13), and a small fraction of the input virus was detectable for the duration of long-term infection. A Gardella gel was also performed to resolve if persisting HSV genomes adopted

the circular conformation characteristic of quiescence (Figure 4.15, Figure 4.16). The results were unable to determine the configuration of V422 in infection of differentiated UW228 cells, however, as the amount of virus present was below the limit of detection by the method used [105]. These results confirmed that HSV V422 genomes could be detected in cultures of differentiated UW228 cells throughout long-term infection, however were unable to indicate if this persisting virus was representative of quiescent infection.

From these results it remains unclear whether HSV V422 infection of differentiated UW228 cells satisfies the definition of quiescence. Following inoculation of this system lytic gene expression and infectious virus disappeared, while viral DNA and low-level TK transcription persisted—a situation consistent with quiescence. However, cell density was also observed to decrease following infection (Figure 4.11) and only a fraction of input viral genomes were retained even three days after infection (Figure 4.13). As such, these results could also describe the majority of the virus being lost from culture through induction of cell death, with a minority of residual genomes persisting. As the Gardella gel was unable to clarify if persisting genomes adopted the circular conformation characteristic of latency, it remains uncertain if the persisting virus is significant. Considering this it was concluded that either quiescent infection of differentiated UW228 cells by HSV V422 was established at a low frequency, or that this system was incompatible for use as a model of HSV latency. The determination between these conclusions was made based on the capacity of the virus to be reactivated.

5.3.2 Reactivation

To assess if differentiated UW228 cells could model reactivation it was determined if HSV V422 genomes present in long-term infection could be induced to replicate when exposed to classical reactivation stresses. Long-term infected cultures were exposed to forskolin, TSA, heat shock, superinfected with UV-inactivated HSV, or transduced with cellular Luman, and monitored for changes in cell morphology and number of viral genome copies (Figure 4.20, Figure 4.21, Figure 4.22). Amplification of HSV DNA was seen after treatment with heat shock, UV-inactivated HSV, and after removal of differentiating agents, with other stress treatments proving toxic to cultures independently from the virus.

An increase in the number of HSV genome copies was detected after treatment with heat shock and after removal of differentiating agents (Figure 4.21), with twofold more viral DNA copies found in cultures exposed to heat stress. The greater viral DNA amplification observed following heat shock is somewhat surprising in light of indications that the VP16 activation domain is necessary for successful stress-induced reactivation [65, 84, 88]. As results have not been reproduced sufficiently however it is not currently possible to determine if the difference between treatments is significant. Additionally, it remains to be determined if viral genome amplification is consistently observed. Spontaneous reactivation may be responsible for the increase in viral DNA, as these events have been observed with the V422 mutant in other systems [84]. Alternatively, the addition of HMBA [136] or withdrawal of NGF from culture media [46] during co-cultivation may have facilitated viral replication, although it has not yet been resolved if UW228 cells possess a functional NGF signaling pathway. These results confirm that the small number of HSV V422 genomes persisting in long-term infection of differentiated UW228 cells retain the ability to re-enter the replicative cycle. Further, HSV V422 can be induced to re-enter the productive cycle by exposure to heat shock and by removal of differentiating agents from culture media. While superinfection with UV-inactivated HSV demonstrated the largest increase in viral DNA the irradiated stock displayed residual replicative capacity (Figure 4.22), obscuring the results of providing wild type VP16 to the quiescent V422 virus.

The reactivation stresses which did not result in an increase in viral DNA proved to be incompatible for use in this system. Both TSA and Luman expression caused rapid and complete cell death (Figure 4.20). As TSA has a well-documented relationship with anti-cancer effects in a wide variety of tumour cell lines, the cell death observed in this treatment group is unsurprising. Based on the functional homology between Luman and HSV VP16 [122], it was hypothesized that the cellular protein may be able to activate the quiescent virus in lieu of wild type VP16. No HSV DNA amplification was observed (Table 4.3), and absence of the small elevation in genome copies detected after Ad.LacZ treatment may be explained by the rapid induction of cell death. Finally, treatment with forskolin did not result in the emergence of infectious virus from differentiated UW228 cultures. This result may be attributable to the V422 mutation, as the

VP16 activation domain has been shown to be required for forskolin-mediated reactivation in the PC-12 system [88]. Alternatively as both forskolin and DBcAMP induce cAMP-dependent signaling, it is possible that the lack of an observed effect may be due to the competing function of these two chemicals, although the extent of the molecular response of the virus following treatment was not tested.

These observations have demonstrated that HSV V422 enters into low frequency quiescence upon infection of differentiated UW228 cells, and that the quiescent virus can be induced to re-enter the replicative cycle. From this it can be concluded that differentiated UW228 cells are therefore able to model the HSV latency-reactivation cycle.

5.4 Use of differentiated medulloblastoma cells in modeling the latency-reactivation cycle

The purpose of this project was to determine if differentiated medulloblastoma cells could provide a cellular environment suitable for investigation of the HSV latency-reactivation cycle. Two medulloblastoma cell lines, ONS-76 and UW228, were differentiated and assessed for their ability to host HSV latency and reactivation. Differentiated ONS-76 cells show promise as a model of HSV reactivation, while differentiated UW228 cells are able to model entry into and exit from quiescent HSV infection. Neither model provides the ideal marriage of human and neuronal factors sought by HSV latency research, and both systems have limitations; the differentiated cells retain characteristics of both neurons and glia, and both cell lines require infection with a viral mutant. Additionally, the frequency with which quiescence was established in the UW228 cell line was not only low, but also highly variable (Figure 4.13, Figure 4.21). Despite these shortcomings, differentiated medulloblastoma cells provide a tool for study of the HSV latency-reactivation cycle that has not as of yet been described. Medulloblastomas are distinct from other differentiated cell models in that they originate from the human CNS, and this provides a means of observing HSV biology from a different cellular perspective. Lastly, this body of work can be used to inform development of future cell culture models based on human neural tumour cell lines.

References

1. Knipe, D.M., et al., eds. *Fields Virology*. 5th ed. 2007, Lippincott Williams & Wilkins. 3177.
2. Howard, M., et al., *Regional distribution of antibodies to herpes simplex virus type 1 (HSV-1) and HSV-2 in men and women in Ontario, Canada.* J Clin Microbiol, 2003. **41**(1): p. 84-9.
3. Karasneh, G.A. and D. Shukla, *Herpes simplex virus infects most cell types in vitro: clues to its success.* Virol J, 2011. **8**: p. 481.
4. Simmen, K.A., et al., *Protein interactions in the herpes simplex virus type 1 VP16-induced complex: VP16 peptide inhibition and mutational analysis of host cell factor requirements.* J Virol, 1997. **71**(5): p. 3886-94.
5. Everett, R.D., et al., *PML contributes to a cellular mechanism of repression of herpes simplex virus type 1 infection that is inactivated by ICP0.* J Virol, 2006. **80**(16): p. 7995-8005.
6. McLean, G., et al., *Identification and characterization of the virion protein products of herpes simplex virus type 1 gene UL47.* J Gen Virol, 1990. **71 (Pt 12)**: p. 2953-60.
7. Mossman, K.L., et al., *Evidence that herpes simplex virus VP16 is required for viral egress downstream of the initial envelopment event.* J Virol, 2000. **74**(14): p. 6287-99.
8. Kwong, A.D., J.A. Kruper, and N. Frenkel, *Herpes simplex virus virion host shutoff function.* J Virol, 1988. **62**(3): p. 912-21.
9. Melchjorsen, J., S. Matikainen, and S.R. Paludan, *Activation and evasion of innate antiviral immunity by herpes simplex virus.* Viruses, 2009. **1**(3): p. 737-59.
10. Boutell, C. and R.D. Everett, *Regulation of alphaherpesvirus infections by the ICP0 family of proteins.* J Gen Virol, 2013. **94**(Pt 3): p. 465-81.
11. Aggarwal, A., et al., *Ultrastructural visualization of individual tegument protein dissociation during entry of herpes simplex virus 1 into human and rat dorsal root ganglion neurons.* J Virol, 2012. **86**(11): p. 6123-37.

12. Miranda-Saksena, M., et al., *Anterograde transport of herpes simplex virus type 1 in cultured, dissociated human and rat dorsal root ganglion neurons.* J Virol, 2000. **74**(4): p. 1827-39.
13. Hafezi, W., et al., *Entry of Herpes Simplex Virus Type 1 (HSV-1) into the Distal Axons of Trigeminal Neurons Favors the Onset of Nonproductive, Silent Infection.* PLoS Pathog, 2012. **8**(5): p. e1002679.
14. Kolb, G. and T.M. Kristie, *Association of the cellular coactivator HCF-1 with the Golgi apparatus in sensory neurons.* J Virol, 2008. **82**(19): p. 9555-63.
15. Lakin, N.D., et al., *Down regulation of the octamer binding protein Oct-1 during growth arrest and differentiation of a neuronal cell line.* Brain Res Mol Brain Res, 1995. **28**(1): p. 47-54.
16. Hagmann, M., et al., *Transcription factors interacting with herpes simplex virus alpha gene promoters in sensory neurons.* Nucleic Acids Res, 1995. **23**(24): p. 4978-85.
17. Nogueira, M.L., et al., *Herpes simplex virus infections are arrested in Oct-1-deficient cells.* Proc Natl Acad Sci U S A, 2004. **101**(6): p. 1473-8.
18. Speck, P.G. and A. Simmons, *Synchronous appearance of antigen-positive and latently infected neurons in spinal ganglia of mice infected with a virulent strain of herpes simplex virus.* J Gen Virol, 1992. **73 (Pt 5)**: p. 1281-5.
19. Thompson, R.L. and N.M. Sawtell, *Replication of herpes simplex virus type 1 within trigeminal ganglia is required for high frequency but not high viral genome copy number latency.* J Virol, 2000. **74**(2): p. 965-74.
20. Proenca, J.T., et al., *A historical analysis of herpes simplex virus promoter activation in vivo reveals distinct populations of latently infected neurones.* J Gen Virol, 2008. **89**(Pt 12): p. 2965-74.
21. Sawtell, N.M., R.L. Thompson, and R.L. Haas, *Herpes simplex virus DNA synthesis is not a decisive regulatory event in the initiation of lytic viral protein expression in neurons in vivo during primary infection or reactivation from latency.* J Virol, 2006. **80**(1): p. 38-50.
22. Bertke, A.S., et al., *A5-positive primary sensory neurons are nonpermissive for productive infection with herpes simplex virus 1 in vitro.* J Virol, 2011. **85**(13): p. 6669-77.

23. Yang, L., C.C. Voytek, and T.P. Margolis, *Immunohistochemical analysis of primary sensory neurons latently infected with herpes simplex virus type 1.* J Virol, 2000. **74**(1): p. 209-17.
24. Dodd, J. and T.M. Jessell, *Lactoseries carbohydrates specify subsets of dorsal root ganglion neurons projecting to the superficial dorsal horn of rat spinal cord.* J Neurosci, 1985. **5**(12): p. 3278-94.
25. Thompson, R.L. and N.M. Sawtell, *The herpes simplex virus type 1 latency-associated transcript gene regulates the establishment of latency.* J Virol, 1997. **71**(7): p. 5432-40.
26. Liebgott, B., *The anatomical basis of dentistry*. 2nd ed2001, St. Louis: Mosby. x, 546 p.
27. Smith, K.T. and J.L. Workman, *Chromatin proteins: key responders to stress.* PLoS Biol, 2012. **10**(7): p. e1001371.
28. Jackson, S.A. and N.A. DeLuca, *Relationship of herpes simplex virus genome configuration to productive and persistent infections.* Proc Natl Acad Sci U S A, 2003. **100**(13): p. 7871-6.
29. Kwiatkowski, D.L., H.W. Thompson, and D.C. Bloom, *The polycomb group protein Bmi1 binds to the herpes simplex virus 1 latent genome and maintains repressive histone marks during latency.* J Virol, 2009. **83**(16): p. 8173-81.
30. Glass, M. and R.D. Everett, *Components of promyelocytic leukemia nuclear bodies (ND10) act cooperatively to repress herpesvirus infection.* J Virol, 2013. **87**(4): p. 2174-85.
31. Newhart, A., et al., *Single-cell analysis of Daxx and ATRX-dependent transcriptional repression.* J Cell Sci, 2012. **125**(Pt 22): p. 5489-501.
32. Cliffe, A.R., D.M. Coen, and D.M. Knipe, *Kinetics of facultative heterochromatin and polycomb group protein association with the herpes simplex viral genome during establishment of latent infection.* MBio, 2013. **4**(1).
33. Proenca, J.T., et al., *An investigation of herpes simplex virus promoter activity compatible with latency establishment reveals VP16-independent activation of immediate-early promoters in sensory neurones.* J Gen Virol, 2011. **92**(Pt 11): p. 2575-85.

34. Chen, Q., et al., *CTCF-dependent chromatin boundary element between the latency-associated transcript and ICP0 promoters in the herpes simplex virus type 1 genome.* J Virol, 2007. **81**(10): p. 5192-201.
35. Shen, W., et al., *Two small RNAs encoded within the first 1.5 kilobases of the herpes simplex virus type 1 latency-associated transcript can inhibit productive infection and cooperate to inhibit apoptosis.* J Virol, 2009. **83**(18): p. 9131-9.
36. Umbach, J.L., et al., *MicroRNAs expressed by herpes simplex virus 1 during latent infection regulate viral mRNAs.* Nature, 2008. **454**(7205): p. 780-3.
37. Javier, R.T., et al., *A herpes simplex virus transcript abundant in latently infected neurons is dispensable for establishment of the latent state.* Virology, 1988. **166**(1): p. 254-7.
38. Flores, O., et al., *Mutational Inactivation of HSV-1 microRNAs Identifies Viral mRNA Targets and Reveals Phenotypic Effects in Culture.* J Virol, 2013.
39. Kim, D.H., et al., *Argonaute-1 directs siRNA-mediated transcriptional gene silencing in human cells.* Nat Struct Mol Biol, 2006. **13**(9): p. 793-7.
40. Rinn, J.L., et al., *Functional demarcation of active and silent chromatin domains in human HOX loci by noncoding RNAs.* Cell, 2007. **129**(7): p. 1311-23.
41. Carpenter, D., et al., *Stable cell lines expressing high levels of the herpes simplex virus type 1 LAT are refractory to caspase 3 activation and DNA laddering following cold shock induced apoptosis.* Virology, 2007. **369**(1): p. 12-8.
42. Perng, G.C., et al., *Virus-induced neuronal apoptosis blocked by the herpes simplex virus latency-associated transcript.* Science, 2000. **287**(5457): p. 1500-3.
43. Jin, L., et al., *Cellular FLIP can substitute for the herpes simplex virus type 1 latency-associated transcript gene to support a wild-type virus reactivation phenotype in mice.* J Neurovirol, 2008. **14**(5): p. 389-400.
44. Chen, X.P., et al., *The relationship of herpes simplex virus latency associated transcript expression to genome copy number: a quantitative study using laser capture microdissection.* J Neurovirol, 2002. **8**(3): p. 204-10.
45. Wang, K., et al., *Laser-capture microdissection: refining estimates of the quantity and distribution of latent herpes simplex virus 1 and varicella-zoster virus DNA in human trigeminal Ganglia at the single-cell level.* J Virol, 2005. **79**(22): p. 14079-87.

46. Wilcox, C.L. and E.M. Johnson, Jr., *Nerve growth factor deprivation results in the reactivation of latent herpes simplex virus in vitro.* J Virol, 1987. **61**(7): p. 2311-5.
47. Camarena, V., et al., *Nature and duration of growth factor signaling through receptor tyrosine kinases regulates HSV-1 latency in neurons.* Cell Host Microbe, 2010. **8**(4): p. 320-30.
48. Theil, D., et al., *Latent herpesvirus infection in human trigeminal ganglia causes chronic immune response.* Am J Pathol, 2003. **163**(6): p. 2179-84.
49. Knickelbein, J.E., et al., *Noncytotoxic lytic granule-mediated CD8+ T cell inhibition of HSV-1 reactivation from neuronal latency.* Science, 2008. **322**(5899): p. 268-71.
50. Jiang, X., et al., *The herpes simplex virus type 1 latency-associated transcript can protect neuron-derived C1300 and Neuro2A cells from granzyme B-induced apoptosis and CD8 T-cell killing.* J Virol, 2011. **85**(5): p. 2325-32.
51. De Regge, N., et al., *Interferon alpha induces establishment of alphaherpesvirus latency in sensory neurons in vitro.* PLoS One, 2010. **5**(9).
52. Vogelbaum, M.A., J.X. Tong, and K.M. Rich, *Developmental regulation of apoptosis in dorsal root ganglion neurons.* J Neurosci, 1998. **18**(21): p. 8928-35.
53. Hunsperger, E.A. and C.L. Wilcox, *Caspase-3-dependent reactivation of latent herpes simplex virus type 1 in sensory neuronal cultures.* J Neurovirol, 2003. **9**(3): p. 390-8.
54. Murray, J.I., et al., *Diverse and specific gene expression responses to stresses in cultured human cells.* Mol Biol Cell, 2004. **15**(5): p. 2361-74.
55. Amelio, A.L., et al., *Deacetylation of the herpes simplex virus type 1 latency-associated transcript (LAT) enhancer and a decrease in LAT abundance precede an increase in ICP0 transcriptional permissiveness at early times postexplant.* J Virol, 2006. **80**(4): p. 2063-8.
56. Neumann, D.M., et al., *In vivo changes in the patterns of chromatin structure associated with the latent herpes simplex virus type 1 genome in mouse trigeminal ganglia can be detected at early times after butyrate treatment.* J Virol, 2007. **81**(23): p. 13248-53.
57. Freeman, M.L., et al., *Psychological stress compromises CD8+ T cell control of latent herpes simplex virus type 1 infections.* J Immunol, 2007. **179**(1): p. 322-8.

58. Kristie, T.M., J.L. Vogel, and A.E. Sears, *Nuclear localization of the C1 factor (host cell factor) in sensory neurons correlates with reactivation of herpes simplex virus from latency.* Proc Natl Acad Sci U S A, 1999. **96**(4): p. 1229-33.
59. Whitlow, Z. and T.M. Kristie, *Recruitment of the transcriptional coactivator HCF-1 to viral immediate-early promoters during initiation of reactivation from latency of herpes simplex virus type 1.* J Virol, 2009. **83**(18): p. 9591-5.
60. Liang, Y., et al., *Inhibition of the histone demethylase LSD1 blocks alpha-herpesvirus lytic replication and reactivation from latency.* Nat Med, 2009. **15**(11): p. 1312-7.
61. Zhao, H., et al., *Activation of the transcription factor Oct-1 in response to DNA damage.* Cancer Res, 2000. **60**(22): p. 6276-80.
62. Du, T., G. Zhou, and B. Roizman, *HSV-1 gene expression from reactivated ganglia is disordered and concurrent with suppression of latency-associated transcript and miRNAs.* Proc Natl Acad Sci U S A, 2011. **108**(46): p. 18820-4.
63. Kim, J.Y., et al., *Transient reversal of episome silencing precedes VP16-dependent transcription during reactivation of latent HSV-1 in neurons.* PLoS Pathog, 2012. **8**(2): p. e1002540.
64. Kushnir, A.S., D.J. Davido, and P.A. Schaffer, *Role of nuclear factor Y in stress-induced activation of the herpes simplex virus type 1 ICP0 promoter.* J Virol, 2010. **84**(1): p. 188-200.
65. Thompson, R.L., C.M. Preston, and N.M. Sawtell, *De novo synthesis of VP16 coordinates the exit from HSV latency in vivo.* PLoS Pathog, 2009. **5**(3): p. e1000352.
66. Suzuki, N., et al., *Mouse Oct-1 contains a composite homeodomain of human Oct-1 and Oct-2.* Nucleic Acids Res, 1993. **21**(2): p. 245-52.
67. Webre, J.M., et al., *Rabbit and Mouse Models of HSV-1 Latency, Reactivation, and Recurrent Eye Diseases.* J Biomed Biotechnol, 2012. **2012**: p. 18.
68. Giordani, N.V., et al., *During herpes simplex virus type 1 infection of rabbits, the ability to express the latency-associated transcript increases latent-phase transcription of lytic genes.* J Virol, 2008. **82**(12): p. 6056-60.
69. Soriano, P., *Generalized lacZ expression with the ROSA26 Cre reporter strain.* Nat Genet, 1999. **21**(1): p. 70-1.

70. Sawtell, N.M., *The probability of in vivo reactivation of herpes simplex virus type 1 increases with the number of latently infected neurons in the ganglia.* J Virol, 1998. **72**(8): p. 6888-92.
71. Stevens, J.G. and M.L. Cook, *Latent herpes simplex virus in spinal ganglia of mice.* Science, 1971. **173**(3999): p. 843-5.
72. Sawtell, N.M. and R.L. Thompson, *Comparison of herpes simplex virus reactivation in ganglia in vivo and in explants demonstrates quantitative and qualitative differences.* J Virol, 2004. **78**(14): p. 7784-94.
73. Kobayashi, M., et al., *A primary neuron culture system for the study of herpes simplex virus latency and reactivation.* J Vis Exp, 2012(62).
74. Danaher, R.J., R.J. Jacob, and C.S. Miller, *Establishment of a quiescent herpes simplex virus type 1 infection in neurally-differentiated PC12 cells.* J Neurovirol, 1999. **5**(3): p. 258-67.
75. Hsu, W.L. and R.D. Everett, *Human neuron-committed teratocarcinoma NT2 cell line has abnormal ND10 structures and is poorly infected by herpes simplex virus type 1.* J Virol, 2001. **75**(8): p. 3819-31.
76. Gimenez-Cassina, A., F. Lim, and J. Diaz-Nido, *Differentiation of a human neuroblastoma into neuron-like cells increases their susceptibility to transduction by herpesviral vectors.* J Neurosci Res, 2006. **84**(4): p. 755-67.
77. Lee, K.S., et al., *Human sensory neurons derived from induced pluripotent stem cells support varicella-zoster virus infection.* PLoS One, 2012. **7**(12): p. e53010.
78. McMahon, R. and D. Walsh, *Efficient quiescent infection of normal human diploid fibroblasts with wild-type herpes simplex virus type 1.* J Virol, 2008. **82**(20): p. 10218-30.
79. Marshall, K.R., et al., *Long-term transgene expression in mice infected with a herpes simplex virus type 1 mutant severely impaired for immediate-early gene expression.* J Virol, 2000. **74**(2): p. 956-64.
80. Preston, C.M., *Reactivation of expression from quiescent herpes simplex virus type 1 genomes in the absence of immediate-early protein ICP0.* J Virol, 2007. **81**(21): p. 11781-9.

81. Preston, C.M. and M.J. Nicholl, *Repression of gene expression upon infection of cells with herpes simplex virus type 1 mutants impaired for immediate-early protein synthesis.* J Virol, 1997. **71**(10): p. 7807-13.
82. Samaniego, L.A., L. Neiderhiser, and N.A. DeLuca, *Persistence and expression of the herpes simplex virus genome in the absence of immediate-early proteins.* J Virol, 1998. **72**(4): p. 3307-20.
83. Halford, W.P., et al., *ICP0, ICP4, or VP16 expressed from adenovirus vectors induces reactivation of latent herpes simplex virus type 1 in primary cultures of latently infected trigeminal ganglion cells.* J Virol, 2001. **75**(13): p. 6143-53.
84. Miller, C.S., R.J. Danaher, and R.J. Jacob, *ICP0 is not required for efficient stress-induced reactivation of herpes simplex virus type 1 from cultured quiescently infected neuronal cells.* J Virol, 2006. **80**(7): p. 3360-8.
85. DeLuca, N.A., A.M. McCarthy, and P.A. Schaffer, *Isolation and characterization of deletion mutants of herpes simplex virus type 1 in the gene encoding immediate-early regulatory protein ICP4.* J Virol, 1985. **56**(2): p. 558-70.
86. Weinheimer, S.P., et al., *Deletion of the VP16 open reading frame of herpes simplex virus type 1.* J Virol, 1992. **66**(1): p. 258-69.
87. Smiley, J.R. and J. Duncan, *Truncation of the C-terminal acidic transcriptional activation domain of herpes simplex virus VP16 produces a phenotype similar to that of the in1814 linker insertion mutation.* J Virol, 1997. **71**(8): p. 6191-3.
88. Danaher, R.J., et al., *C-terminal trans-activation sub-region of VP16 is uniquely required for forskolin-induced herpes simplex virus type 1 reactivation from quiescently infected-PC12 cells but not for replication in neuronally differentiated-PC12 cells.* J Neurovirol, 2013. **19**(1): p. 32-41.
89. Stow, N.D. and E.C. Stow, *Isolation and characterization of a herpes simplex virus type 1 mutant containing a deletion within the gene encoding the immediate early polypeptide Vmw110.* J Gen Virol, 1986. **67 (Pt 12)**: p. 2571-85.
90. Thompson, R.L. and N.M. Sawtell, *Evidence that the herpes simplex virus type 1 ICP0 protein does not initiate reactivation from latency in vivo.* J Virol, 2006. **80**(22): p. 10919-30.

91. Marino, S., *Medulloblastoma: developmental mechanisms out of control.* Trends Mol Med, 2005. **11**(1): p. 17-22.
92. Roussel, M.F. and M.E. Hatten, *Cerebellum development and medulloblastoma.* Curr Top Dev Biol, 2011. **94**: p. 235-82.
93. Bhatia, B., et al., *Hedgehog-mediated regulation of PPARgamma controls metabolic patterns in neural precursors and shh-driven medulloblastoma.* Acta Neuropathol, 2012. **123**(4): p. 587-600.
94. Poschl, J., et al., *Constitutive activation of beta-catenin in neural progenitors results in disrupted proliferation and migration of neurons within the central nervous system.* Dev Biol, 2013. **374**(2): p. 319-32.
95. Park, K.C., K. Shimizu, and T. Hayakawa, *Interferon yield and MHC antigen expression of human medulloblastoma cells and its suppression during dibutyryl cyclic AMP-induced differentiation: do medulloblastoma cells derive from bipotent neuronal and glial progenitors?* Cell Mol Neurobiol, 1998. **18**(5): p. 497-507.
96. Stockhammer, G., et al., *Inhibition of proliferation and induction of differentiation in medulloblastoma- and astrocytoma-derived cell lines with phenylacetate.* J Neurosurg, 1995. **83**(4): p. 672-81.
97. Li, X.N., et al., *Phenylbutyrate and phenylacetate induce differentiation and inhibit proliferation of human medulloblastoma cells.* Clin Cancer Res, 2004. **10**(3): p. 1150-9.
98. Agholme, L., et al., *An in vitro model for neuroscience: differentiation of SH-SY5Y cells into cells with morphological and biochemical characteristics of mature neurons.* J Alzheimers Dis, 2010. **20**(4): p. 1069-82.
99. Lopes, F.M., et al., *Comparison between proliferative and neuron-like SH-SY5Y cells as an in vitro model for Parkinson disease studies.* Brain Res, 2010. **1337**: p. 85-94.
100. Lam, Q., et al., *Herpes simplex virus VP16 rescues viral mRNA from destruction by the virion host shutoff function.* EMBO J, 1996. **15**(10): p. 2575-81.
101. Cai, W.Z. and P.A. Schaffer, *Herpes simplex virus type 1 ICP0 plays a critical role in the de novo synthesis of infectious virus following transfection of viral DNA.* J Virol, 1989. **63**(11): p. 4579-89.

102. Yao, F. and P.A. Schaffer, *An activity specified by the osteosarcoma line U2OS can substitute functionally for ICP0, a major regulatory protein of herpes simplex virus type 1.* J Virol, 1995. **69**(10): p. 6249-58.
103. Valderrama, X. and V. Misra, *Novel Brn3a cis-acting sequences mediate transcription of human trkA in neurons.* J Neurochem, 2008. **105**(2): p. 425-35.
104. Vetter, G., et al., *miR-661 expression in SNAI1-induced epithelial to mesenchymal transition contributes to breast cancer cell invasion by targeting Nectin-1 and StarD10 messengers.* Oncogene, 2010. **29**(31): p. 4436-48.
105. Decker, L.L., G.J. Babcock, and D.A. Thorley-Lawson, *Detection and discrimination of latent and replicative herpesvirus infection at the single cell level in vivo.* Methods Mol Biol, 2001. **174**: p. 111-6.
106. Whitehouse, A., *Gardella gel analysis to detect Herpesvirus saimiri episomal DNA.* Cold Spring Harb Protoc, 2011. **2011**(12): p. 1524-6.
107. Wang, Q., et al., *Resveratrol promotes differentiation and induces Fas-independent apoptosis of human medulloblastoma cells.* Neurosci Lett, 2003. **351**(2): p. 83-6.
108. Yu, L.J., et al., *Inhibition of STAT3 expression and signaling in resveratrol-differentiated medulloblastoma cells.* Neoplasia, 2008. **10**(7): p. 736-44.
109. Muragaki, Y., et al., *Nerve growth factor induces apoptosis in human medulloblastoma cell lines that express TrkA receptors.* J Neurosci, 1997. **17**(2): p. 530-42.
110. Tamura, K., et al., *Expression of major histocompatibility complex on human medulloblastoma cells with neuronal differentiation.* Cancer Res, 1989. **49**(19): p. 5380-4.
111. Keles, G.E., et al., *Establishment and characterization of four human medulloblastoma-derived cell lines.* Oncol Res, 1995. **7**(10-11): p. 493-503.
112. Friedman, H.S., et al., *Establishment and characterization of the human medulloblastoma cell line and transplantable xenograft D283 Med.* J Neuropathol Exp Neurol, 1985. **44**(6): p. 592-605.
113. Habauzit, D., et al., *Effects of estrogens and endocrine-disrupting chemicals on cell differentiation-survival-proliferation in brain: contributions of neuronal cell lines.* J Toxicol Environ Health B Crit Rev, 2011. **14**(5-7): p. 300-27.

114. Martin, T.F. and R.N. Grishanin, *PC12 cells as a model for studies of regulated secretion in neuronal and endocrine cells.* Methods Cell Biol, 2003. **71**: p. 267-86.
115. Miller, C., et al., *Herpesvirus quiescence (QIF) in neuronal cells VI: Correlative analysis demonstrates usefulness of QIF-PC12 cells to examine HSV-1 latency, reactivation and genes implicated in its regulation.* Curr Eye Res, 2003. **26**(3-4): p. 239-48.
116. Joshi, H.C. and D.W. Cleveland, *Differential utilization of beta-tubulin isotypes in differentiating neurites.* J Cell Biol, 1989. **109**(2): p. 663-73.
117. Katsetos, C.D., et al., *Class III beta-tubulin isotype (beta III) in the adrenal medulla: III. Differential expression of neuronal and glial antigens identifies two distinct populations of neuronal and glial-like (sustentacular) cells in the PC12 rat pheochromocytoma cell line maintained in a Gelfoam matrix system.* Anat Rec, 1998. **250**(3): p. 351-65.
118. Schimmelpfeng, J., K.F. Weibezahn, and H. Dertinger, *Quantification of NGF-dependent neuronal differentiation of PC-12 cells by means of neurofilament-L mRNA expression and neuronal outgrowth.* J Neurosci Methods, 2004. **139**(2): p. 299-306.
119. Gardella, T., et al., *Detection of circular and linear herpesvirus DNA molecules in mammalian cells by gel electrophoresis.* J Virol, 1984. **50**(1): p. 248-54.
120. Danaher, R.J., et al., *Heat stress activates production of herpes simplex virus type 1 from quiescently infected neurally differentiated PC12 cells.* J Neurovirol, 1999. **5**(4): p. 374-83.
121. Danaher, R.J., et al., *Histone deacetylase inhibitors induce reactivation of herpes simplex virus type 1 in a latency-associated transcript-independent manner in neuronal cells.* J Neurovirol, 2005. **11**(3): p. 306-17.
122. Lu, R. and V. Misra, *Potential role for luman, the cellular homologue of herpes simplex virus VP16 (alpha gene trans-inducing factor), in herpesvirus latency.* J Virol, 2000. **74**(2): p. 934-43.
123. Fang, K.M., et al., *Mps one binder 2 gene upregulation in the stellation of astrocytes induced by cAMP-dependent pathway.* J Cell Biochem, 2012. **113**(9): p. 3019-28.
124. Fedoroff, S., et al., *Astrocyte cell lineage. III. The morphology of differentiating mouse astrocytes in colony culture.* J Neurocytol, 1984. **13**(1): p. 1-20.

125. Aravalli, R.N., et al., *Differential apoptotic signaling in primary glial cells infected with herpes simplex virus 1.* J Neurovirol, 2006. **12**(6): p. 501-10.
126. Dix, R.D., L. Hurst, and R.W. Keane, *Herpes simplex virus type 1 infection of mouse astrocytes treated with basic fibroblast growth factor.* J Gen Virol, 1992. **73 (Pt 7)**: p. 1845-8.
127. Hancock, M.H., et al., *Herpes simplex virus VP16, but not ICP0, is required to reduce histone occupancy and enhance histone acetylation on viral genomes in U2OS osteosarcoma cells.* J Virol, 2010. **84**(3): p. 1366-75.
128. Hancock, M.H., J.A. Corcoran, and J.R. Smiley, *Herpes simplex virus regulatory proteins VP16 and ICP0 counteract an innate intranuclear barrier to viral gene expression.* Virology, 2006. **352**(1): p. 237-52.
129. Yousefi, I., *Selective activation of unfolded protein response (UPR) by herpes simplex virus type 1 (HSV-1) in permissive and non permissive cells*, in *Veterinary Microbiology*2011, University of Saskatchewan: Saskatoon.
130. Johnson, P.A., M.J. Wang, and T. Friedmann, *Improved cell survival by the reduction of immediate-early gene expression in replication-defective mutants of herpes simplex virus type 1 but not by mutation of the virion host shutoff function.* J Virol, 1994. **68**(10): p. 6347-62.
131. Krisky, D.M., et al., *Deletion of multiple immediate-early genes from herpes simplex virus reduces cytotoxicity and permits long-term gene expression in neurons.* Gene Ther, 1998. **5**(12): p. 1593-603.
132. Ace, C.I., et al., *Construction and characterization of a herpes simplex virus type 1 mutant unable to transinduce immediate-early gene expression.* J Virol, 1989. **63**(5): p. 2260-9.
133. Kramer, M.F. and D.M. Coen, *Quantification of transcripts from the ICP4 and thymidine kinase genes in mouse ganglia latently infected with herpes simplex virus.* J Virol, 1995. **69**(3): p. 1389-99.
134. Rodahl, E. and L. Haarr, *Analysis of the 2-kilobase latency-associated transcript expressed in PC12 cells productively infected with herpes simplex virus type 1: evidence for a stable, nonlinear structure.* J Virol, 1997. **71**(2): p. 1703-7.

135. Mehta, A., et al., *In situ DNA PCR and RNA hybridization detection of herpes simplex virus sequences in trigeminal ganglia of latently infected mice.* Virology, 1995. **206**(1): p. 633-40.
136. McFarlane, M., J.I. Daksis, and C.M. Preston, *Hexamethylene bisacetamide stimulates herpes simplex virus immediate early gene expression in the absence of trans-induction by Vmw65.* J Gen Virol, 1992. **73 (Pt 2)**: p. 285-92.